

A SIMPLIFIED NUCLEAR REACTOR
CORE SIMULATOR MODEL

A THESIS

Presented to
The Faculty of the Division
of Graduate Studies

By
Douglas Kenneth Vogt

In Partial Fulfillment
of the Requirements for the Degree
Master of Science in Nuclear Engineering

Georgia Institute of Technology

October, 1975

A SIMPLIFIED NUCLEAR REACTOR
CORE SIMULATOR MODEL

Approved:

R. W. Carlson, Chairman

J. D. Clement

C. B. Woodhall

Date approved by Chairman: Jan 6, 1976

ACKNOWLEDGMENTS

Throughout this work I have received advice and support from fellow employees at Nuclear Assurance Corporation. Discussions with Paul Schutt in the area of fuel cycle economics and Dr. Yoon Chang on the development and use of fuel cycle correlations were extremely helpful. Jim Hobbs of NAC and Joe Kearney of the Office of Management and Budget provided valuable insight into the methods used in existing core simulator models. As work progressed, the suggestions of Dave Pitts and especially John-Paul Renier dealing with computer software utilization proved very useful.

I am grateful for the guidance offered by Dr. Joseph Clement and Colman B. Woodhall of the thesis committee. I am especially grateful to Dr. Roger Carlson, the committee chairman. I am also thankful for John Kenton's expert editing of the final thesis draft, and for Sharon Butler's careful preparation of the final manuscript.

Finally, I am indebted to my parents for their support and guidance through the years.

TABLE OF CONTENTS

	Page
ACKNOWLEDGMENTS.	ii
LIST OF TABLES	iv
LIST OF ILLUSTRATIONS.	v
Chapter	
I. INTRODUCTION.	1
II. EVOLUTION OF CURRENT METHODS.	10
Core Depletion Analyses	
Fuel Cycle Cost Analyses	
Summary	
III. DEVELOPMENT OF CORE SIMULATOR MODEL	32
Algorithms	
Correlations	
Model	
IV. FUEL FAILURES-FUEL COSTS--A PARAMETRIC ANALYSIS .	57
BIBLIOGRAPHY	81

LIST OF TABLES

Table	Page
1. XPLOAD* Core Depletion Results.	54
2. XPLOAD Batchwise Cycle-by-Cycle Burnups	55
3. XPLOAD Cycle Length Predictions	56
4. SNUPPS Reactor Fuel Cycle Plan.	59
5. Representative Refueling Plans Investigated . . .	60
6. Cost Data Used in CINCAS Analyses	73

*The computer code described in this thesis.

LIST OF ILLUSTRATIONS

Figure	Page
1. Core Simulator Predicted Cycle Lengths and SNUPPS Cycle Lengths.	39
2. Core Simulator Predicted Cycle-by-Cycle Batchwise Energy Production and SNUPPS Data . . .	41
3. Core Simulator Predicted Discharge Exposures and SNUPPS Discharge Exposures.	42
4. U-235 Enrichment as a Function of Initial Enrichment and Fuel Exposure.	45
5. Uranium Weight as a Function of Fuel Exposure . .	46
6. Fissile Plutonium Content as a Function of Initial Enrichment and Fuel Exposure.	47
7. Fuel K-infinity as a Function of Initial Enrichment and Fuel Exposure.	48
8. XPLOAD Flow Chart	50
9. FUSE Logic.	52
10. The Effect of the Early Discharge of Twelve Low Enrichment One-Cycle Fuel Assemblies on Cycle Energy Production	63
11. The Effect of Early Discharge Batch Size on Subsequent Fuel Cycle Lengths for the Early Replacement of One-Cycle Low Enrichment Fuel Assemblies.	65
12. The Effect of the Early Discharge of Twelve High Enrichment One-Cycle Fuel Assemblies on Cycle Energy Production	67
13. The Effect of Early Discharge Batch Size on Subsequent Fuel Cycle Lengths for the Early Replacement of One-Cycle High Enrichment Fuel Assemblies.	68

Figure	Page
14. The Effect of the Early Discharge of Twelve High Enrichment Two-Cycle Fuel Assemblies on Cycle Energy Production.	69
15. The Effect of the Early Discharge Batch Size on Subsequent Fuel Cycle Lengths for the Early Replacement of Two-Cycle High Enrichment Fuel Assemblies	70
16. The Effect of Fuel Exposure on Net Fuel Assembly Cost.	74
17. The Effect of Premature Fuel Discharge Batch Size on Case Fuel Costs.	76
18. The Effect of Premature Fuel Discharge on Cycle Energy Costs	77

CHAPTER I

INTRODUCTION

The original decision to build commercial nuclear power plants was based upon the economic potential of fission produced power. In the mid 1950's, it became apparent that nuclear fission could be an economically attractive alternative to fossil fueled electrical generating stations. It was at this time that construction of the first commercial demonstration plants utilizing the nuclear fission process as a heat source for electric power generation was begun.

The first commercial nuclear power plants were one-of-a-kind installations. Yankee Rowe, the pioneer commercial pressurized water reactor, was designed by Westinghouse.¹ The reactor core consisted of 76 stainless steel clad fuel assemblies containing slightly enriched uranium. Each fuel assembly was enclosed in a stainless steel channel to control the reactor core coolant flow distribution, to provide assembly structural strength, and to provide a bearing surface for the cruciform control rods used for short-term power control and reactor shutdown.

The first core of Yankee Rowe was designed for a life of 8,000 MWD/MTU. At the end of the first cycle of operation, the entire first core was discharged, and a new

slightly-enriched uranium fueled core was inserted. The second core was designed for multi-cycle irradiation with a three-region out-in, fuel shuffling scheme; the centermost fuel region was discharged from the reactor at the end of each cycle of operation.

The first Babcock and Wilcox nuclear power reactor was Indian Point 1,² a 270 MWe plant utilizing fossil-fired superheaters. The first core of Indian Point 1 was radically different from any other fuel loading in a commercial light water reactor in that it was designed to breed uranium-233 from thorium. The first core fuel consisted of 120 fuel assemblies utilizing highly enriched uranium and thorium as fuel. The original plan was to convert fertile thorium-232 to uranium-233 and recycle the bred uranium in the reactor to take advantage of its superior neutronic value as compared to the plutonium produced in slightly enriched uranium fuel. However, problems arose with reactor operations, and commercial facilities capable of reprocessing and refabricating the irradiated uranium-thorium fuel mixture were not developed. At the end of the first cycle of operation, Indian Point 1 discharged the entire uranium-thorium fuel loading and inserted a fresh core consisting of slightly enriched uranium fuel assemblies.

Combustion Engineering's first commercial power reactor was Palisades.³ The fuel design for Palisades was also significantly different from that used in other pressurized

water reactors. This unique fuel design was the result of the use of cruciform control rods for supplemental reactivity control and reactor shutdown.

The first Boiling Water Reactors designed by General Electric reflected rapidly evolving design variations. Dresden 1,⁴ the first commercial Boiling Water Reactor, utilized 464 fuel assemblies. Each assembly contained thirty-six slightly enriched uranium fuel rods in a 6x6 array. The Big Rock Point⁵ and Humboldt Bay⁶ reactors came on line shortly after Dresden 1. Although these reactors employed different fuel designs, they did make use of a standardized fuel shuffling scheme. At a typical refueling, approximately one-fourth of the fuel would be replaced. Fresh fuel would be loaded on the core periphery, and previously irradiated fuel would be scatter-loaded in the core interior.

As these first reactors began to produce electricity in the early 1960's, it became apparent that future United States nuclear generating capacity would consist of Light Water Reactors. Studies were conducted and various experimental reactors¹⁰⁻²⁰ utilizing a wide variety of coolants and moderators, various fissionable materials as fuels, and several fertile materials were constructed, but further development was not pursued. By the mid-to-late 1960's four Light Water Reactor vendors had developed Nuclear Steam Supply Systems. Fuel designs while still evolving, were becoming standardized for each reactor vendor. The basic

techniques utilized to design, fabricate, and reprocess fuel for these Light Water Reactors were known and being established in commercial practice. The technology associated with the Light Water Reactor and its fuel cycle was moving from a first-of-a-kind to a mature status.

During the evolution of the nuclear industry in the 1950's and 1960's, economic studies performed in support of nuclear power plants were quite simple.²¹⁻²³ The main factor prohibiting detailed analyses of nuclear fuel costs was the lack of a firm commitment to nuclear power and the resulting uncertainties in the requirements for and the cost of design and fabrication of reactor fuel. In addition, there was comparatively little in-reactor operating experience with nuclear fuels, and hence only limited experience to draw upon in evaluating the potential mechanical and nuclear life of fuel under reactor operating conditions.

The first nuclear fuel cost studies involved back-of-the-envelope calculations which provided rough estimates of nuclear power costs. The methods used in these first cost calculations grew out of methods used to calculate fossil fuel costs. The first estimates of nuclear power cost were based primarily on the cost of the U-235 consumed in the fission process, a readily available cost item as the AEC was the sole owner and supplier of uranium. The lack of additional cost information was due to major uncertainties in the technologies which would be utilized to fabricate and

reprocess commercial reactor fuel when large scale production was achieved. As the nuclear industry grew, the uncertainties relating to nuclear components and fuel design as well as fuel fabrication were slowly resolved until, as the commercial light water reactor industry matured, the information required for detailed nuclear power cost evaluations was at hand.

As the technology associated with nuclear power matured, competition developed within the industry. By the late 1960's, the four major reactor vendors were actively marketing light water reactors and associated nuclear fuel. In addition, by 1970 there were three independent companies offering to provide fuel fabrication and associated services for commercial light water reactors.²⁴ As the number of nuclear fuel fabricators increased, the market became quite competitive. Competition resulted in major differences in scope as well as terms and conditions of proposed contracts for fuel fabrication and related services.²⁵⁻²⁸

Fuel fabricators would offer bids for fuel fabrication often containing options for supply of uranium ore and conversion to UF_6 prior to enrichment with a combined price for both components of the fuel cycle. Escalation clauses varied from fuel fabricator to fuel fabricator as did payment schedules. In addition to the varying contract terms, the cost of capital for individual utilities varied greatly.²⁶⁻²⁸ For each fabrication contract, a given utility would be faced

with evaluating a broad spectrum of component costs and payment terms. In addition, vendors would offer different reloading schemes for the same or different cycle energy productions. These reloading schemes would involve variations in fuel assembly reload enrichment or reload batch size, or both, adding still more variations to contract proposals. In order to compare the energy costs associated with the various offerings, detailed nuclear fuel cost analyses were necessary.

The need for these fuel cost studies led to the development of two types of computer models. The first type²⁹⁻³⁷ was the coupled core depletion and economics model which was used to predict fuel cycle energy production with sufficient accuracy to be used in long-range economic studies.

The second type of model³⁸ involved a detailed fuel cycle cost calculation where the cycle energy production, batch-wise energy production, the cost of various fuel components, and interest costs, were input quantities determined in other calculations.

Core depletion codes developed for use in the first type of fuel cycle cost studies were typically one or two dimensional, few-group neutron diffusion theory models or non-dimensional few-group depletion models.³⁹⁻⁴⁴ Generally, these depletion models resulted from simplification of computer codes used in design work.

The second type of cost analyses generally were

applied to determine the fuel cycle cost of the final design and required data from a separate core depletion model to simulate core energy production. The energy production data was transmitted to fuel cycle cost codes as part of the total input data required to calculate the nuclear fuel cost.

Since these nuclear fuel cycle cost codes were one of the bases for selecting fuel fabricators for multi-million dollar fuel fabrication contracts, there was tremendous incentive to employ the second type of model to optimize fuel cycle costs. However, it was readily apparent that running complex nuclear depletion codes for the large variety of enrichments and fuel loading patterns was too expensive and time consuming for such optimizations. Because of this, much of the recent work in the area of fuel cycle economics and optimization has been in the area of development of core depletion models that are simple and fast-running.⁴³⁻⁵⁴ Very little effort has been exerted toward improving the accuracy of the first type of fuel cycle cost calculation, resulting in a "one-sided" approach to the problem.

At the present time, fuel cycle simulators of the first type are used by all fuel fabricators for the preparation of proposals that reflect optimum feasible fuel reloading schemes. Similar methods are also utilized by several utilities for determining optimum system loading strategies and additionally as long-range planning tools for system growth. However, the final design is governed by the second

type of fuel cycle cost model.

The computational methods currently used with core simulators vary from simplified multi-dimensional, multi-group diffusion theory calculations to point reactor calculations. The diffusion theory core simulator models are fairly complex and rely upon basic data (i.e. neutron cross-sections, fuel core shuffling schemes, etc.). Past works^{43-45, 52-54} have shown that for the degree of accuracy required for many fuel cycle cost studies, the amount of detail generated by these codes is not required. Because of this, point depletion algorithms and pseudo-point depletion algorithms have been developed for fuel cycle cost analyses. These models vary in both their computational speed and in their ability consistently and accurately to predict fuel cycle energy production and costs.

Although several of the core simulators which have been developed do permit quite reliable predictions of core energy production, their only applications have involved either fuel cycle optimization, long-range system loading studies, or related works. The core simulator models which have been developed to date are not suitable as short-range planning tools or for evaluating perturbations to normal fuel management schemes. Experience with operating nuclear power plants has shown that short-term reactor operations will vary significantly from long-range plans of operation.⁵⁵⁻⁵⁶ These variations in reactor operations will often result in

variations in fuel management plans. In the past there have been many major perturbations to fuel management plans, including: partial refuelings to prolong fuel cycle length; refueling before the nuclear end-of-cycle to utilize refueling windows; and the premature discharge of fuel assemblies due to cladding failure, design deficiencies, and faulty fabrication techniques. The only methods currently available for evaluating this spectrum of problems require the use of few-group neutron diffusion theory. If it is desired to perform parametric analyses for any of these problems, the number of man-weeks and computer-hours required would be significant.

In order effectively to produce this type of parametric analysis cost data with a minimum expenditure of manpower and computer cost, use of a simplified core simulator model is desirable to predict core energy production. This work deals with the requirements for a simplified simulator model, and the methods used in the development of such a model beginning with a history of the methods currently available for fuel management studies in Chapter II. Here, the emphasis is placed on the evolution of assumptions which have significantly simplified fuel management studies. In Chapter III, the algorithms for a core simulator model are developed based upon a stated set of assumptions. Chapter IV contains the results of a parametric study of a perturbation of reactor operation and notes pertinent conclusions.

CHAPTER II

EVOLUTION OF CURRENT METHODS

Core Depletion Analysis

Core depletion models, presently used for fuel cycle cost analysis differ greatly in the calculational methods they employ and in their predictive capabilities. Existing models typically fall into one of two general categories. The first category⁵⁷⁻⁶⁴ includes few-group two and three-dimensional neutron diffusion theory depletion models which are used throughout the nuclear industry as tools for reactor core design. These models give fairly accurate results for a broad range of problems, but require considerable computational time and effort. In addition, current design codes provide a degree of detail which is not necessary in most fuel management studies. To meet the requirements of fuel management studies, a second group of computer codes has been developed.⁶⁵⁻⁷⁰ Fuel management codes presently in use include simpler one and two dimensional few-group diffusion theory depletion models, pseudo-dimensional models, and point depletion models. Core simulators based on these models may require extensive input and are often limited to specific problem types.

The first generation of depletion codes was typified

by the CANDLE,⁶⁸ TURBO,⁶⁹ and DRACO⁷⁰ computer codes developed at Westinghouse for the naval reactor program. Each of these codes could be conveniently divided into two separate sections. The first section solved the few-group neutron diffusion equation with spatially dependent coefficients and the second section performed the time dependent depletion of the heavy isotopes. A numerical solution to the diffusion equation was used to determine the neutron flux at each point of the reactor core under consideration. Spatially dependent coefficients in the diffusion equation were based on fitted few-group parameters and spatially-dependent material densities which could be altered to account for depletion caused by neutron absorption at each point or to include the effects of the radioactive decay of the material during each interval of time. The second section of these depletion codes contained the coupled, first-order, linear differential depletion equations describing the growth and decay of the densities of various isotopes at each point in the reactor core. Values of the neutron flux at each point were obtained from the solution of the diffusion equations and were assumed to remain constant within the time interval during which the material isotopic densities were calculated by the solution of the depletion equations in the second section of the code. The initial isotopic densities were obtained from the material density input data and the solution of the depletion equations provided the

material densities for the next calculation of the spatial fluxes from the diffusion equations in the first section of the code.

The CANDLE code utilizes a two or four energy-group one-dimensional diffusion theory technique for the prediction of the spatially dependent neutron flux.

The depletion algorithm used in CANDLE has served as a forerunner for subsequent Westinghouse depletion codes. The method is based upon the solution of linear differential equations representing heavy metal, Xenon, Samarium, and lumped fission product concentrations.

TURBO and DRACO are two and three-dimensional codes respectively. TURBO has been used extensively in the nuclear industry for fuel management studies. The current version of TURBO treats either the R-Z or X-Y geometry using a coarse-mesh finite difference method for the calculation of the spatially dependent neutron flux. The depletion calculation is similar to that used in CANDLE. DRACO is essentially a three-dimensional version of TURBO.

Early studies at Westinghouse using these codes showed that although the use of three-dimensional depletion codes was desirable to obtain accurate estimates of lifetime and information about power distributions as a function of time, their use was generally too costly to be justified on an ongoing basis.⁷¹⁻⁷² An alternative approach to the solution of the three-dimensional problem was the use of a

two-dimensional (X-Y) code in conjunction with an axial flux synthesis code. To accomplish this, Westinghouse developed ZIP,⁷³ which utilized TURBO to predict the spatial flux distribution in the X-Y plane and CANDLE for axial flux synthesis. The techniques used for flux synthesis are described in detail in the literature.⁷³⁻⁷⁵ Briefly, the Westinghouse ZIP synthesis of the axial flux involved generating an effective fuel concentration at each axial point and depleting the core axially, independent of the previous X-Y depletion calculation. The radial buckling (B_R^2) from the two-dimensional calculation computed by the TURBO X-Y planar solution was used in developing a radial leakage term for the CANDLE axial synthesis calculation. The axial buckling (B_Z^2) calculated by CANDLE was then compared with that used in the previous ZIP X-Y planar calculation. Complex, iterative techniques⁷⁴⁻⁷⁵ were developed to produce agreement between the different eigenvalues (λ_R and λ_Z) predicted by the TURBO and CANDLE calculations. Studies with ZIP showed that the separation of the axial and radial modes did not produce significantly different numerical results from those predicted by three-dimensional codes. This showed that the axial exposure distribution and the radial exposure distribution are essentially separable as is commonly assumed for the analytic solution of partial differential equations. Although there are variations in the numerical methods used for the solutions of both the diffusion equations and depletion

equations, one and two-dimensional diffusion theory depletion calculations similar to those used in these codes constitute the basis for most current fuel management studies.

For core analyses of a BWR, the axial variation of neutron flux is influenced by the water density (void distribution) and burnable poison distribution in a given fuel assembly. The effects of thermal-hydraulic feedback on BWR core physics require a two or three-dimensional nuclear calculation with coupled thermal-hydraulic feedback. Early analyses of BWR cores showed that here also multi-group codes with thermal-hydraulic feedback required excessive computer time to perform meaningful analyses. To reduce the magnitude of the calculational problem, a 1.5-group absorption probability model, FLARE,⁷⁶ was developed by General Electric. The technique used in FLARE was to solve the neutron balance equation assuming no thermal neutron diffusion. This assumption reduced the two group equations to a single equation which could be solved quickly.

In order to further simplify the simulation of BWR cores, the end-of-cycle Haling power distribution has been developed to reduce the dimensionality of the depletion problem and to simplify the depletion procedure in fuel management studies.^{43,48-50} The Haling principle⁷⁷ postulates that for any given set of end-of-cycle conditions, the power peaking factor is maintained at a minimum when the global

power shape does not change during the cycle. End-of-cycle conditions may be considered to consist of such parameters as the exposure of the fuel, the presence or absence of residual burnable poison, or control rods remaining in core at the end of any operating cycle. The optimum power shape is thus determined by the end-of-cycle conditions and the consistent power and exposure distributions. One method of computing this power shape is to iterate between power distribution and the effect of exposure on nodal k -infinity. By first assuming a power shape, the value of the nodal k -infinity at the end of a given cycle can be determined. This k -infinity distribution can then be used in a diffusion theory calculation to determine the end-of-cycle power shape. Repetition of this procedure will eventually yield a power distribution and end-of-cycle reactivity (k -infinity) which are consistent. This converged solution represents the optimal Haling power shape.

Actual design to the Haling distribution in a BWR would require the use of distributed burnable poisons which would exactly offset the effects of fuel burnup and result in operation at a given power distribution (i.e. the Haling power distribution) throughout a given cycle. In a PWR, the radial power distribution is essentially constant throughout a given cycle because of the absence of control rods from the core during normal operations. Hence the Haling power distribution is a good approximation for PWR depletion analyses.

The Haling principle has been utilized both to reduce the dimensionality of the BWR simulation problem and to allow one-step depletion of a reactor core for fuel management studies. Soodak and Nakache⁴⁸ at Gulf United Nuclear Fuels Corporation, Forker and Specker⁴³ at TVA, and Snyder and Lewis⁵⁰ have all developed absorption probability models using the Haling principle to simplify the depletion calculations. In each of these instances, the neutron balance equation was solved using 1.5-group theory. Depletion of core excess reactivity during the cycle was accomplished in one step by using the Haling principle.

At those installations where 1.5-group absorption probability theory or few group diffusion theory have been used extensively for fuel management studies, tabulations of pertinent lattice physics data have been utilized to speed calculations.^{43,48-50} In these cases either correlations or tabular interpolation of cell code calculation results served as basic information.

Cell codes⁷⁸⁻⁸¹ were developed to generate the necessary physics data for core depletion calculations. These codes were originally designed as microscopic burnup physics calculations concerned with the accurate calculation of reaction rates and fuel compositions as a function of burnup at a point or in a cell representative of a given portion of a core. In current practice this information is used to generate the group average cross-sections required

for multi-group diffusion theory calculations. Because cell codes involved elements of small physical size and are either non-dimensional or one-dimensional, very detailed and accurate calculations can be performed without extensive use of computational time.

One of the more widely used non-spatially dependent neutron spectrum calculation codes is LEOPARD.⁸⁰ This code generates physics parameters for a homogeneous unit cell and performs a nuclear calculation using the slowing down program MUFT,⁸² a B-1 approximation to the transport equation and a 172 thermal energy group point calculation with SUFOCATE.⁸³ In order to yield more meaningful analyses, heterogeneity correction factors are used by the code. The code has a fuel depletion option which permits the use of plutonium, uranium or thorium fuels. Xenon and samarium effects are treated using a methodology similar to that of CANDLER. Other fission products are lumped into one pseudo-element. By using a non-dimensional calculation, LEOPARD permits a fast calculation of the neutron spectrum and desired reactor physics parameters.

Problems arise with LEOPARD calculations when spatially dependent effects become important,⁸⁴⁻⁸⁵ notably during depletion problems. The inability to deal with the spatial dependence of uranium consumption, or the effects of self shielding on plutonium production and consumption will give errors in both cross-sections and reactivity values calculated

by any point code. At higher exposures, where these effects are more pronounced, the errors which are introduced will become larger.

In order to accurately account for spatial effects in cell calculations, the unit cell code LASER⁸¹ was developed. This cell code relies on the code MUFT for the neutron slowing down calculation and the one-dimensional integral transport theory code THERMOS⁸⁶ for calculation of the thermal neutron flux distribution. The epithermal and fast energy ranges utilize 50 energy groups and the thermal range includes 35 groups. Fission products are separated into Xe-135, Sm-149, and one lumped pseudo-fission product. The one-dimensional theory approach to the thermal flux in LASER provides an extremely good approximation to the physical problem under study. LASER benchmark calculations have been performed for hot cell examination results of Yankee Rowe fuel.⁸⁵ These calculations showed that the heavy metal isotopic spatial distribution predicted by LASER agreed quite well with hot cell examination results giving added support to the code's predictive capabilities.

Methods of reducing the dimensionality of the Pressurized Water Reactor core simulation problem have been examined by Naft and Sesonske⁴⁰ at Purdue University. For the analysis of a two-dimensional (X-Y plane) problem, a two-dimensional analytical solution and a local augmentation factor. The local augmentation factor was chosen to

represent the material properties of a given fuel assembly plus its nearest neighbors. In their study, Naft and Sesonske found that a linear combination of the material buckling ($B^2 = \frac{k_\infty - 1}{M^2}$) of a given fuel assembly and the material bucklings of adjacent fuel assemblies would provide an adequate augmentation factor. Utilizing this correction factor with a one-dimensional treatment of the power distribution provided excellent agreement with two-dimensional diffusion theory power distribution calculations.

Earlier, more general fuel management studies at Battelle Northwest Labs had utilized core average (or point) models to provide rapid depletion analyses codes. One of the more widely used point codes was ALTHAEA,³⁹ a few-group code which could simulate one of two refueling strategies--batch or graded. The simulation of batch refueling was based on two assumptions. The first was that the fuel is shuffled during the irradiation so that each fuel element would see the same neutron flux over the same period. The second assumption was that neutrons produced in excess of those needed to maintain the chain reaction were absorbed by an idealized control system which did not change the neutron spectrum. In this instance, the reactivity-limited lifetime was reached when the excess reactivity calculated by the code just compensated for neutron leakage. The excess reactivity during irradiation was assumed to be absorbed in the control system so that k-effective was equal to unity

during the irradiation.

In the graded mode, the reactor fueling was arranged so that the excess neutrons were absorbed in fuel elements deficient in neutron production. Since the excess reactivity generally varies approximately linearly with exposure, the average k -infinity of all fuel in the reactor would remain above the minimum k -infinity condition for essentially twice as long as in a batch mode analysis. For the analysis of a graded cycle, it was assumed that excess neutrons would flow to the depleted fuel regions and that the neutron energy spectrum was the same for all fuel in the reactor. This spectrum was the average spectrum for the entire fuel element composition. This was equivalent to irradiating fuel at a constant flux level in a constant neutron spectrum throughout the burnup. The reactivity-limited lifetime of a fuel element was reached when the total number of neutrons produced since startup was equal to the number of neutrons absorbed in the fuel plus the number lost by leakage or otherwise not accounted for during burnup.

The use of a point depletion code for fuel management studies introduces basic assumptions related to core average quantities, which limit the applicability of results. In order to eliminate some of these inadequacies, the code PROTEUS⁸⁷ was developed to extend the results from a point depletion code to make them more compatible with the results of diffusion theory calculations. The primary purpose of this

code was to represent more accurately the time-dependent burnup of the fuel by adjusting the irradiation time scale. The code adjusted the time scale by first determining the flux level that would give the same average specific power with a constant flux for some specific terminal value of k -infinity. The code would then construct a graded irradiation time scale based on the principle that the product of the time and graded flux was constant. Although the addition of an extension to a point code did help to improve the prediction of the time-varying effects of irradiation, the spatially-dependent effects of neutron flux and neutron spectrum could not be represented in the detail afforded by one and two-dimensional depletion codes. Because of this lack of detail, the calculations of the PROTEUS/ALTHAEA code system were only utilized for generalized fuel cycle cost studies.

While point codes based on few-group depletion theory generally did not yield power production information of sufficient accuracy for fuel management simulation, the heavy metal isotopic data which they predicted was often quite accurate. In early studies, few-group depletion codes were used to develop correlations of heavy metal isotopic data. These isotopic correlations have been used to provide consistency checks for more detailed reactor physics calculations and for post-irradiation reprocessing results. Similar correlations have been obtained empirically from

spent fuel reprocessing operations and have in many instances provided more accurate predictions than detailed design code results.

The development of pseudo-dimensional point depletion codes began with the requirement for fast-running depletion algorithms for fuel cycle optimization studies. The first of these optimization studies was done by Wall and Fenech⁴⁵ at MIT. Depletion calculations were first performed using FEVER,⁶⁵ a one-dimensional, few-group diffusion theory depletion code. For their studies, it was assumed that the fuel composition could be expressed solely by the burnup for a given fuel batch. To compute fuel cycle costs, the masses of the fuel inserted and removed at each refueling were necessary. These masses were calculated from the burnups of individual fuel regions. The only information required for the optimization was the transformation of the fuel in the course of one core lifetime as a function of the initial fuel composition and core arrangement. The interim behavior of the reactor as a whole during this lifetime was of no consequence providing constraints on power peaking were not violated. For the purposes of the Wall-Fenech optimization study, the system behavior was predicted by polynomial curves fitted to the results of many FEVER calculations. The end result was a set of expressions for the resultant end-of-life fuel composition, distribution and maximum power peaking during life as functions of the initial fuel composition and

core fuel arrangement. The expressions which were developed were valid over a range of fuel exposures from 0 to 20,000 MWD/MTU. Each reloading pattern was considered separately and the FEVER results were fitted to polynomial functions over the limited regions corresponding to a given situation. However, several reloading patterns gave absurd power distributions, which were totally unacceptable for a realistic reactor, and eventually, only four refueling patterns merited consideration.

Similar techniques have been used by Rhodes⁵¹ at VEPCO, Kearney and Mason⁵² at MIT, Stover and Sesonske⁵³ at Purdue, and Fagan and Sesonske⁵⁴ at Purdue in optimization studies. In each of these instances, the polynomial curves describing the reactor state functions only provided adequate representation for a limited set of operating conditions and generally only one type of reactor. Each of these investigations utilized correlations to predict heavy metal isotopic compositions which, although varying somewhat in form, gave results which were not dependent on the individual situations being analyzed as were the other reactor state functions such as fuel exposure, peaking factors, and cycle lengths. This finding has been confirmed in other similar studies.⁸⁸⁻⁹⁰

At Westinghouse, Henderson and Bauhs utilized a wealth of operating experience from Westinghouse plants to develop a more generalized core simulator model which was

not restricted by the correlations utilized in its algorithms as previous efforts had been. Their computer model was comprised of five modules, two of which were utilized in core depletion analyses. The first depletion module determined cycle-by-cycle batch burnups for the batch sizes and enrichments selected. Input to this module consisted of initial feed enrichments, initial fuel region loadings, and a description of the fuel cycling scheme. The module calculated the weighted average reactivity of the core as a function of the burnup and when the value of the reactivity was equal to the end-of-life value for an equilibrium cycle, the cycle end point was reached.

The effect of power distribution on burnup was accounted for by the concept of burnup sharing. The burnup-sharing of each batch in each cycle was calculated using a mathematical model based on a correlation of data from operating Westinghouse plants and detailed data from nuclear design calculations. This concept was justified on the basis of the consistent out-in refueling strategy used at each refueling for Westinghouse plants.

Batchwise exposures calculated by the first module were passed to a second module which predicted heavy metal isotopics as a function of fuel design parameters, batch size, initial enrichment, and fuel assembly exposure. This module utilized a library of isotopic compositions of fuel at various burnups, enrichments, and a combination of fuel

design parameters. Linear interpolation or extrapolation was used in these physics data banks.

While the predictive capabilities and accuracy of this integrated computer package made it desirable, the large amount of information required for the physics data library would make development of a similar model a monumental undertaking.

Fuel Cycle Cost Analyses

There are currently two types of fuel cycle cost codes available; codes for calculating the actual cost of generating power from nuclear fuel at operating nuclear reactors,³⁸ and codes for predicting the cost of generating power for proposed fuel cycles for nuclear power plants.²⁹⁻³⁷ The basic accounting methods which utilities use to calculate nuclear fuel costs are set forth by the FPC⁹¹ (Federal Power Commission). Regulation by the FPC leaves little leeway in the basic calculational methods which utilities may use for fuel cost calculations for operating nuclear power plants. In evaluating the cost of power at operating facilities, procurement prices, payment schedules, time varying cost of capital, and time varying rates of energy production must be accurately represented. For the purposes of evaluating fuel costs from proposed fuel cycle plans, this degree of detail is neither available nor necessary.⁹²

The first set of industry guidelines for calculational methods to be used for projecting nuclear power costs were

developed by Kaiser Engineering⁹³ for the Atomic Energy Commission in 1960. These guidelines were based on the government leasing special nuclear material to utilities at a lease rate of 4.75% of the value of the contained material. The utility had no concern with materials procurement. The only contracting obligation was to arrange for fuel fabrication. During irradiation, the utility would pay for the fissile material consumed in the production of energy. When fuel was discharged, the utility would arrange for shipment of the fuel to a government facility where it would be reprocessed. After reprocessing, the government retained the special nuclear material. These material and cash flows served as the basis for the calculational methods used in early fuel cycle economics calculations.

With the advent of private ownership of nuclear fuel materials in 1972, and the development of nuclear power as an increasingly widely accepted economic alternative for electric utility system capacity additions, there arose a need for consistent, accurate methods for calculating nuclear fuel costs. At that time, the computer programs which were available either had serious limitations with regard to their flexibility to represent accurately fuel offerings (i.e. private ownership of fuel) or the basic algorithms which they employed had too many approximations. The shortcomings of previously developed computer codes led to the development of a number of fuel cycle economics codes for

fuel cycle cost predictions. The methodology used in these computer codes was generally based on guidelines presented in a study by NUS Corporation⁹² for the Atomic Energy Commission.

Since the fuel cycle cost information predicted by these methods was utilized primarily for bid evaluation, the principal concern was with the fuel cost magnitudes, differences, and working capital requirements. The primary purpose of these fuel cycle cost codes was to utilize a consistent costing methodology so that fuel cost differences would only be a function of basic design and inherent material, process, or service cost differences.

The current generation of fuel cycle cost codes uses fairly standardized accounting methodologies for calculating cash flows. Approximations are generally involved in developing working capital requirements, present-worthing cash flows, and allocating expense and inventory costs. If an evaluation deals with the magnitude of fuel cost variations, most currently accepted fuel cycle codes will prove adequate.

One of the more flexible cost codes in terms of required input, calculational methods, and output edits is CINCAS.³⁷ Although the use of CINCAS is restricted to Light Water Reactors operating with either slightly enriched uranium or mixed oxide fuel, it has seen considerable use in financial, industrial, and university environments; and is considered as one of the "standard" fuel cost codes in the

industry.

CINCAS calculates the fuel contribution to total electrical generating cost. The expense calculations within CINCAS are performed on a fuel batch basis where a fuel batch is comprised of a group of one or more fuel assemblies. Each fuel batch experiences the same burnup, has the same initial and final isotopic compositions, and undergoes fuel cycle steps at the same times. For each batch of fuel evaluated, the following items are input:

1. Unit prices of each process in the fuel cycle; including: U_3O_8 purchase, conversion to UF_6 , UF_6 enrichment, fabrication of UF_6 into finished fuel assemblies, storage and shipping of spent fuel, reprocessing and reconversion.
2. Types, times, and amounts of progress payments.
3. Time intervals associated with the movement of the batch through the fuel cycle.
4. Interest rates for inventory calculations.
5. Batch fuel weights as a function of burnup.
6. Projected energy production schedule.

The philosophy in CINCAS is to allocate total cost incurred by a batch from start to finish of the fuel cycle to that time during which the batch produced saleable electricity. All costs are assigned to one or more cost categories. There are five direct, or expense, cost categories, and four inventory cost categories: uranium expense, fabrication expense, shipping expense, reprocessing

expense, reconversion expense, uranium inventory, plutonium inventory, fabrication inventory, and post-irradiation inventory.

Direct cost items are allocated based on heat production during a given month. Inventory costs are obtained by applying an appropriate interest rate to the average monthly inventory value. Preirradiation costs incurred as uranium and fabrication progress payments for the batch are treated as interest during construction and are assigned to beginning inventory values. Features of CINCAS include:

1. Monthly calculation of dollar costs and mass inventory on a batch and case basis for each month of a period.
2. Variable monthly batch energy production and plant efficiencies, and allocation of costs by heat production.
3. Provision for reinserted batches.
4. Input of batch fuel weights of uranium and plutonium on a burnup-dependent basis.
5. A general formula for the unit price of enriched uranium which allows for variable feed and tails enrichments, costs of feed, chemical conversion, separative work, and losses in conversion and fabrication.
6. Calculation of costs in units of dollars, cents per million BTU's, or mills/kilowatt-hour.
7. Present worthing and levelizing calculations.
8. Provision for escalation of fabrication progress payments due to labor and material price increases.

Many of the major weaknesses of CINCAS arise from the assumptions which permit accounting on a batch-by-batch basis. For example: utility purchases of raw materials are made to cover system requirements, not individual fuel batches, therefor utilities will often procure materials without a particular end use need in mind. Interest rates for inventory calculations will vary on a temporal basis, not a fuel batch basis. The calculational methods used within CINCAS assume that nuclear material is expensed as it is consumed, and that the revenue from the power which is produced is received as the nuclear material is consumed. These assumptions prevent an exact representation of fuel costs. However, CINCAS is useful as a tool for engineering economic studies in which the primary concern is determining relative cost variations due to changes in various components of fuel cycle cost or changes due to differences in fuel batch energy production.

Summary

Current core depletion analysis methods range from pseudo-point models to point models to one, two, and three-dimensional diffusion theory models. Those models which rely on basic physics calculations (the data for which is generated by cell codes), are capable of analyzing a broad spectrum of fuel management alternatives at the expense of computational time. Those models which utilize nondimensional calculations either fail to take into account in-reactor

spatial affects or in taking those affects into account limit their problem-solving capability.

Fuel cycle economics codes have developed into two well-defined groups: codes for predicting actual generating costs, and codes for forecasting future generating costs that make use of simplifying assumptions to permit quicker calculation. When relative differences in fuel cost are the primary concern of an analysis, most of the current fuel cycle economics forecasting codes will provide adequate results.

CHAPTER III

DEVELOPMENT OF CORE SIMULATOR MODEL

There is a large class of fuel management problems which current computer codes do not address. These problems typically involve the parametric analysis of the effect of many perturbations to a reactor's fuel management plan resulting in energy and/or fuel cost fluctuations. These perturbations result from changes in fuel cycle length, unscheduled fuel discharges, and changes in reload fuel enrichment. For current standardized reactor fuel management plans, analysis of these problems requires a simplified core simulator model and a coupled fuel cycle economics code. In order to analyze many different problems, the core simulator should be quick, accurate, and easy to use. The model should be flexible to provide the ability to represent a broad variety of fuel management alternatives. In addition, the model should utilize a simple, easy-to-prepare set of input data to facilitate the rapid preparation of input information to permit the rapid study of crucial problems. And of course if it is to come into wide use, the fuel cycle economics code must be well accepted by the industry.

Algorithms

The core simulator developed in this work was based on

the application of the Haling principle to the radial power distribution in a pressurized water reactor. In order to permit the application of the Haling principle to predict the exposure distribution and to allow flexibility in analyses without compromising calculation speed or precision, the following assumptions were made:

1. Cycle length can be predicted by knowing the full-power excess reactivity at end-of-cycle. This permits a unique definition of cycle end state and allows flexibility in choosing the end-of-cycle condition.

2. The radial power shape will remain constant throughout a given cycle of operation. This allows a one-step depletion of the reactor core by the Haling principle.

3. The radial power shape can be adequately predicted by fuel assembly location and beginning-of-cycle reactivity. This assumption forms the basis for a fuel batch energy allocation algorithm.

4. K-infinity and heavy metal nuclide concentrations can be adequately represented as functions of fuel batch average initial enrichment and exposure, giving a quick but accurate method of calculating these critical parameters.

The algorithm used to predict energy production in the reactor core consists of a cycle length predictor and a method of allocating energy production to individual fuel batches. The cycle length predictor relies upon a relatively simple technique which utilizes a weighted average value of

core k -infinity to determine cycle length. First an estimate of the cycle length is made using data derived from vendor bid specifications contained in Nuclear Assurance Corporation's fuel-trac data base.⁹⁴ Available information has shown that to a first approximation, fuel cycle length is linearly proportional to reactivity depletion during a given cycle. Thus,

$$B_c = C \cdot (\bar{k}_\infty^i - \bar{k}_\infty^f) \quad (4-1)$$

where B_c is the core average exposure in MWD/kgU, C is an empirically determined constant, \bar{k}_∞^i is the core average k -infinity at the beginning of life, and \bar{k}_∞^f is the core average k -infinity at the end of life. By a trial and error methodology, the value of 80 was chosen for C . This value of C typically permitted the calculation of B_c to within $\pm 5\%$ of the desired value as a first guess. After an initial guess of B_c was made, the core was depleted to end-of-cycle conditions and the end-of-cycle value of k -infinity was recalculated for the depleted core utilizing a weighted average of fuel batch k -infinities. This value of k -infinity was compared with the desired end-of-cycle k -infinity and if the difference between the two was greater than a specified tolerance, the cycle length was reestimated using a fixed point iteration technique.⁹⁵ It was found that using this technique, convergence to within $.0001\% \Delta k_\infty$ could be obtained

within a maximum of six iterations.

By utilizing the Haling principle for the power distribution of a reactor core, the core can be depleted using a single time step, once the core power distribution is known. For the core simulator, the power distribution was approximated by fuel assembly k-infinity. For a modified "out-in" fuel shuffling technique, this approximation will reasonably well represent the power-sharing in the core central region. In the core periphery, leakage effects are dominant in determining the power distribution. Because of this, the power density of a region being burned for the first time was assumed to be constant. These assumptions agree well with observations from operating reactors.

The algorithm to determine the batch burnup increment during operation was based on allocation of the cycle energy production on the basis of the assumed power distribution. After the calculation of cycle energy production in MWD/MTU, a constant proportion of the cycle energy was allocated to the fuel assemblies in the region defined by the core periphery. For the problems under study, the energy production was found to be adequately represented by the following expression

$$B_p = .7454 \cdot B_c \quad (4-2)$$

for first cores and

$$B_p = .9047 \cdot B_c \quad (4-3)$$

for subsequent cycles. Where B_p is the burnup in MWD/kgU of the core periphery region, for the current cycle, and B_c is the core average exposure in MWD/kgU for the current cycle of operation. These expressions are based upon analyses of periphery region fuel exposures contained in fuel cycle plans in Nuclear Assurance Corporation's fuel-trac data base. First core loadings for the reactors in the analysis utilized burnable poison rods in selected peripheral region fuel assemblies at the beginning of the first fuel cycle. These burnable poison rods reduce the power production in those assemblies containing them. During the first cycle, the burnable poison material is depleted, and at the end of the first core, the burnable poison rods are discharged. Therefore, the peripheral fuel region in the first cycle should contain a "burnup penalty" to allow for burnable poison depletion during the first cycle of operation. This burnup penalty appears as the difference in leading coefficients in equations 4-2 and 4-3. After the determination of the peripheral region fuel exposure, the average burnup of all fuel in the core central region is calculated from the following expression derived from an energy balance for the reactor core:

$$B_i = (B_c \cdot (N_p + N_i) - B_p \cdot N_p) / N_i \quad (4-4)$$

where B_i is the average burnup of the core inner region, B_c is the core average burnup, B_p is the outer fuel region exposure, N_p is the number of fuel assemblies in the core periphery, and N_i is the number of fuel assemblies in the core inner region. The average exposure of the core inner region was then divided among the inner region fuel assemblies based on a Haling power/burnup distribution based on beginning-of-cycle k -infinity:

$$B_b = B_i \frac{k_{\infty}^b}{\bar{k}_{\infty}^i} \quad (4-5)$$

where B_b is the burnup of the fuel in batch b , B_i is the burnup of the core inner region, k_{∞}^b is the value of k -infinity for fuel batch b , and \bar{k}_{∞}^i is the average value of k -infinity in the core central region.

To check the validity of the cycle length predictor, the core simulator was utilized to predict cycle lengths for a proposed refueling for a current reactor vendor standard fuel cycle offering. The example chosen was a Standardized Nuclear Utility Power Plant Syndicate (SNUPPS) Reactor. For the purposes of this calculation, the end-of-cycle reactivity was assumed to correspond to the inverse of the leakage correction term to the four-factor formula for reactor critically,⁹⁶

$$k_{\infty}^f = 1 + M^2 B^2 \quad (4-6)$$

where k_{∞}^f is the end-of-life reactivity, M^2 is the migration area, and B^2 is the critical buckling of the reactor system. Previous LASER calculations had shown that M^2 was essentially constant for the range of fuel exposures and initial enrichments utilized in Pressurized Water Reactors. The value predicted by LASER was 61.0 cm^2 . The critical buckling for a right cylinder is given by:

$$B^2 = \left(\frac{2.405}{R} \right)^2 + \left(\frac{\pi}{H} \right)^2 \quad (4-7)$$

where B is the critical buckling, R is the equivalent core radius, and H is the equivalent core height.

Utilizing the dimensions of the SNUPPS reactor core, the critical buckling for the reactor was found to be $2.774 \times 10^{-4} \text{ cm}^2$. This value of critical buckling yields an end-of-cycle k -infinity of 1.017. It was necessary to account for the non-uniformity of fuel-loading and its effect on reactor core end-of-cycle reactivity. For the SNUPPS reactor fuel loading plan, this effect was assumed to be $.01\% \Delta k_{\infty}$ giving an end-of-cycle k -infinity value of 1.027. Using this end-of-cycle k -infinity value, cycle lengths were calculated for the Westinghouse SNUPPS reactor. The maximum deviation from the Westinghouse predicted value of cycle-length was 1.8% as is shown in Figure 1.

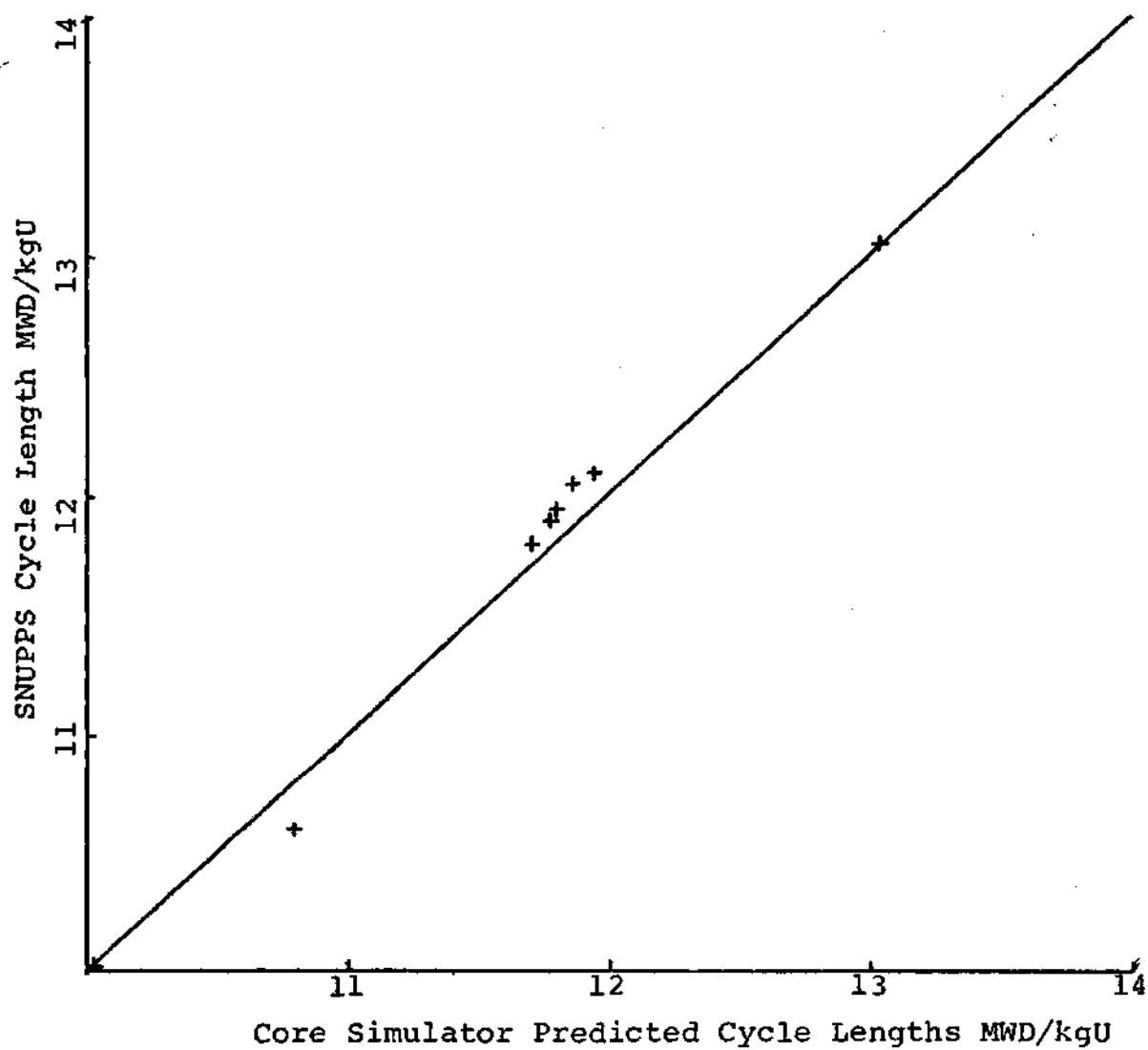


Figure 1. Core Simulator Predicted Cycle Lengths and SNUPPS Cycle Lengths

The method of calculating batch exposures also gave excellent agreement with the fuel cycle offering for the SNUPPS reactor. As seen in Figures 2 and 3, the cycle-by-cycle batchwise burnups agreed to within 5.4% of the Westinghouse proposal values, and the batch discharge exposures agreed to within 1.4%. These differences are well within the current IAEA objectives⁹⁷ for computational techniques of $\pm 2-5\%$ for cycle length predictions and $\pm 2\%$ for batch discharge exposures.

Development of Correlations

In order to predict k-infinity and heavy metal isotopic data as a function of exposure, core cell depletion analyses were run using LASER. The core cell simulated by LASER was a representative core cell of a Westinghouse 15 x 15 rod array fuel assembly. Cell depletion analyses were run for initial U-235 enrichments ranging from 1.5 w/o to 3.5 w/o with cell exposures ranging from 0 to 35 MWD/kgU. The depletion analyses were performed for a core cell having a constant boron concentration of 500 ppm operating at the core average linear heat rate. Constant boron concentrations and heat rates were utilized to permit a relatively quick depletion of the core cell. It would be expected that these approximations to actual core operating conditions would produce heavy metal isotopic data and k-infinity data which would vary from those predicted by more precise cell calculations in which boron concentrations and heat rates

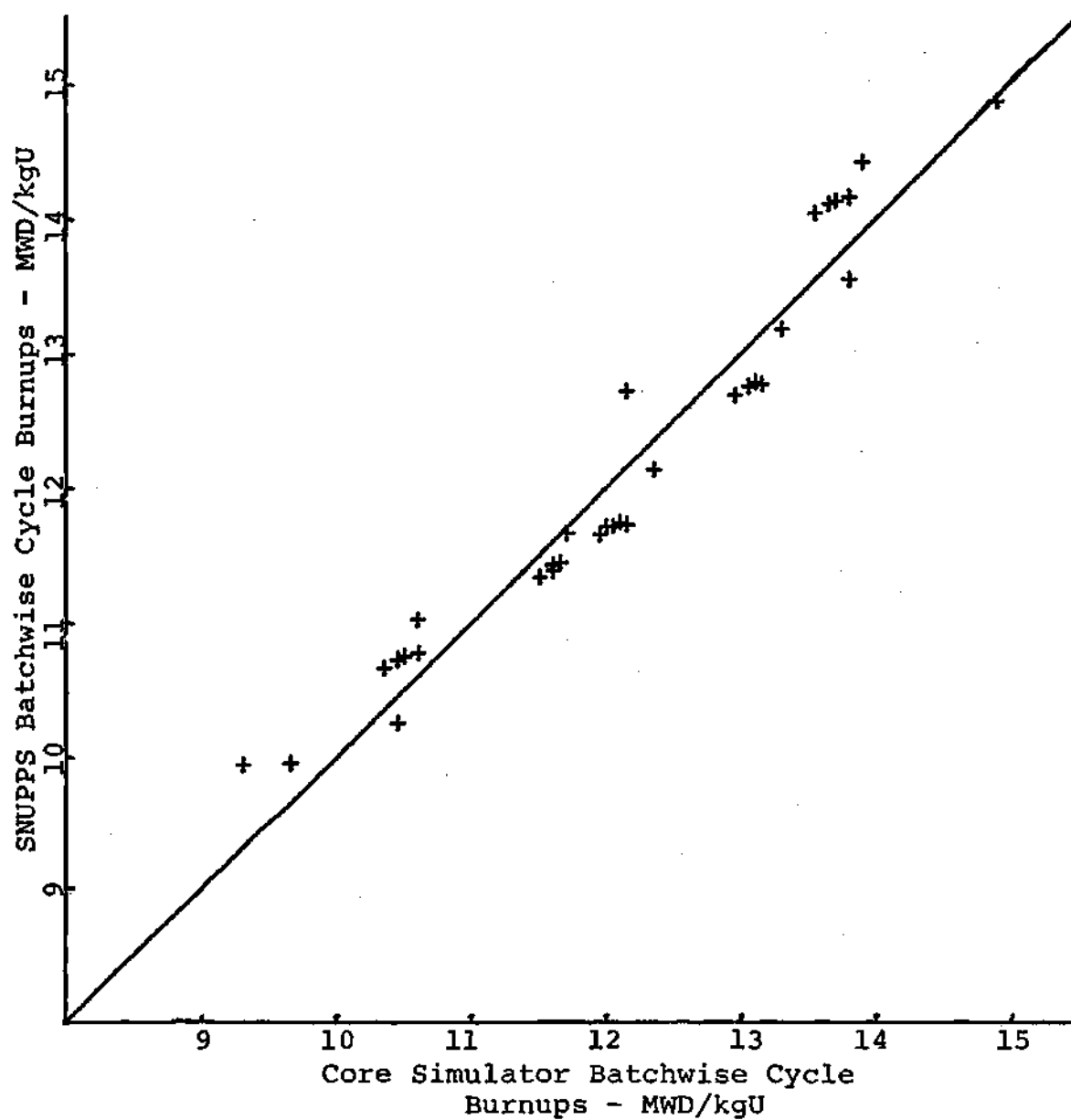


Figure 2. Comparison of Core Simulator Predictions of Cycle by Cycle Batchwise Energy Production

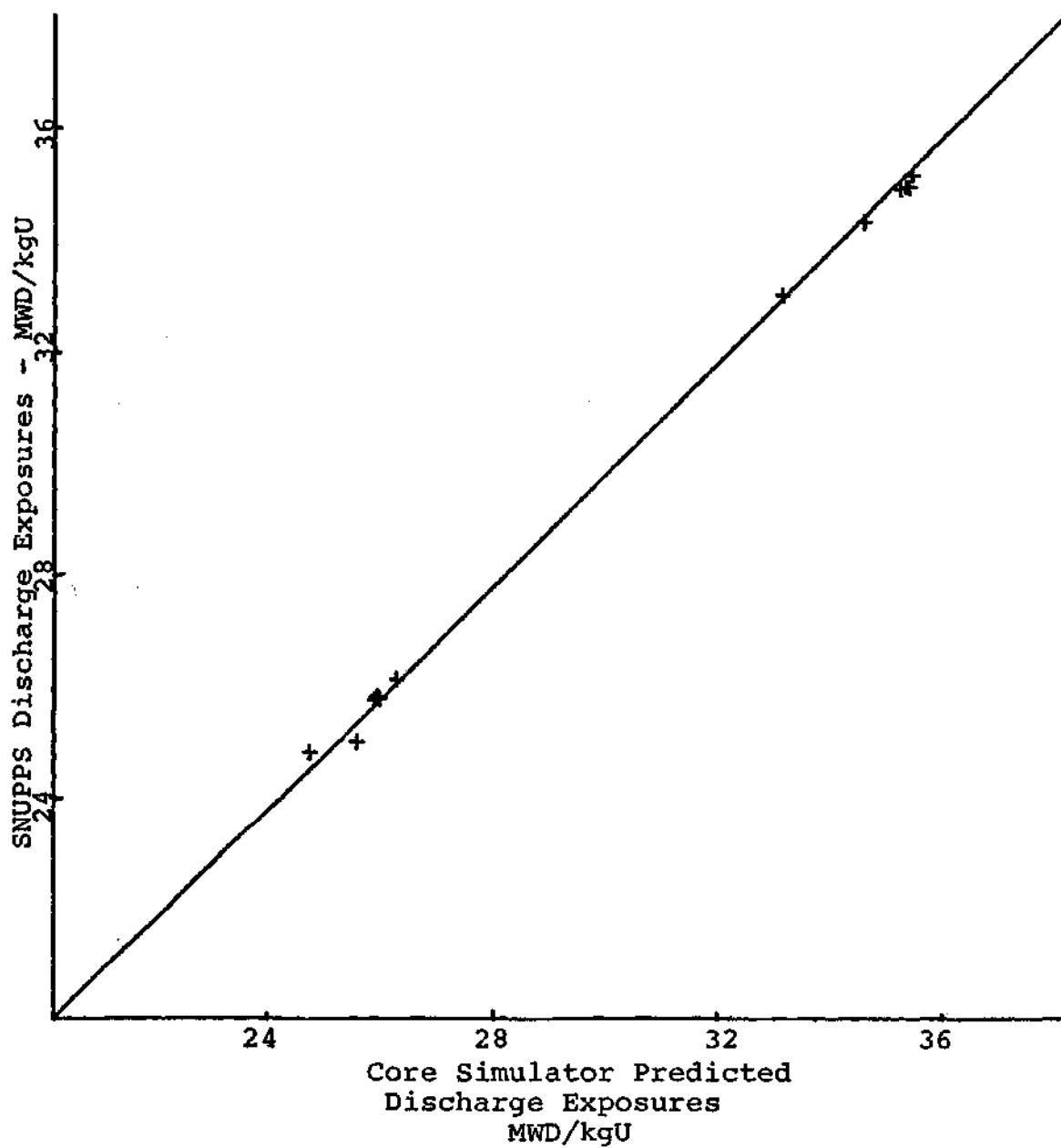


Figure 3. Core Simulator Predicted Discharge Exposures and SNUPPS Discharge Exposures

were varied reflecting actual reactor operations. The parameters most severely affected by this variation should be those which are most sensitive to changes in the thermal neutron spectrum. The LASER output for constant boron concentration and constant heat rate was compared with previous calculations in which the boron concentration was allowed to vary with exposure. The previous calculations⁹⁸ had utilized a boron concentration sawtooth which approximated the varying boron concentration which would exist in a power reactor. It was found that the plutonium concentration was the parameter most sensitive to the variations in neutron spectrum caused by varying boron concentrations. The fissile plutonium content for the uniform boron content depletion case was found to be consistently lower than that calculated using the boron sawtooth by a factor of 1.06.

The LASER heavy metal data output consisted of atom densities as functions of initial enrichment and exposure. These were converted to weight percent of initial metal, and in this form the data was utilized as input to a multiple regression analysis computer program.⁹⁹ Heavy metal isotopics were fitted to a function of the general form.

$$F(E_i, B) = F(E_i, 0) +$$

$$(a_{11} + a_{12} \cdot E_i + a_{13} \cdot E_i^2) \cdot B +$$

$$(a_{21} + a_{22} \cdot E_i + a_{23} \cdot E_i^2) \cdot B^2$$

where E_i is the initial fuel U-235 w/o, B is the fuel exposure in MWD/kgU, and $f(E_i, B)$ represents the heavy metal concentration for the fuel of a given initial enrichment E_i at a given exposure B , and the a_{ij} , are constants determined by a regression analysis routine. The heavy metal isotopic concentrations predicted by the correlations were within 5% of the values produced by the LASER calculation.

Results of the LASER calculations were also used to generate a correlation to represent the infinite multiplication factor, k -infinity, as a function of initial enrichment and exposure. In order to obtain a high degree of accuracy in the k -infinity correlation, the regression analysis program was used to generate a correlation of the form

$$\begin{aligned}
 f(E_i, B) = & a_{00} + a_{01} \cdot E_i + a_{02} \cdot E_i^2 + a_{03} \cdot E_i^3 \\
 & + (a_{10} + a_{11} \cdot E_i + a_{12} \cdot E_i^2) \cdot B \\
 & + (a_{20} + a_{21} \cdot E_i + a_{22} \cdot E_i^2) \cdot B^2 \\
 & + (a_{30} + a_{31} \cdot E_i + a_{32} \cdot E_i^2) \cdot B^3 \\
 & + (a_{40} + a_{41} \cdot E_i + a_{42} \cdot E_i^2) \cdot B^4.
 \end{aligned}$$

This functional form permitted the correlation of k -infinity to within .0025% dk/k over the range of exposures and initial enrichments contained in the LASER calculation. Figures 4 through 7 compare LASER predicted values with the curves

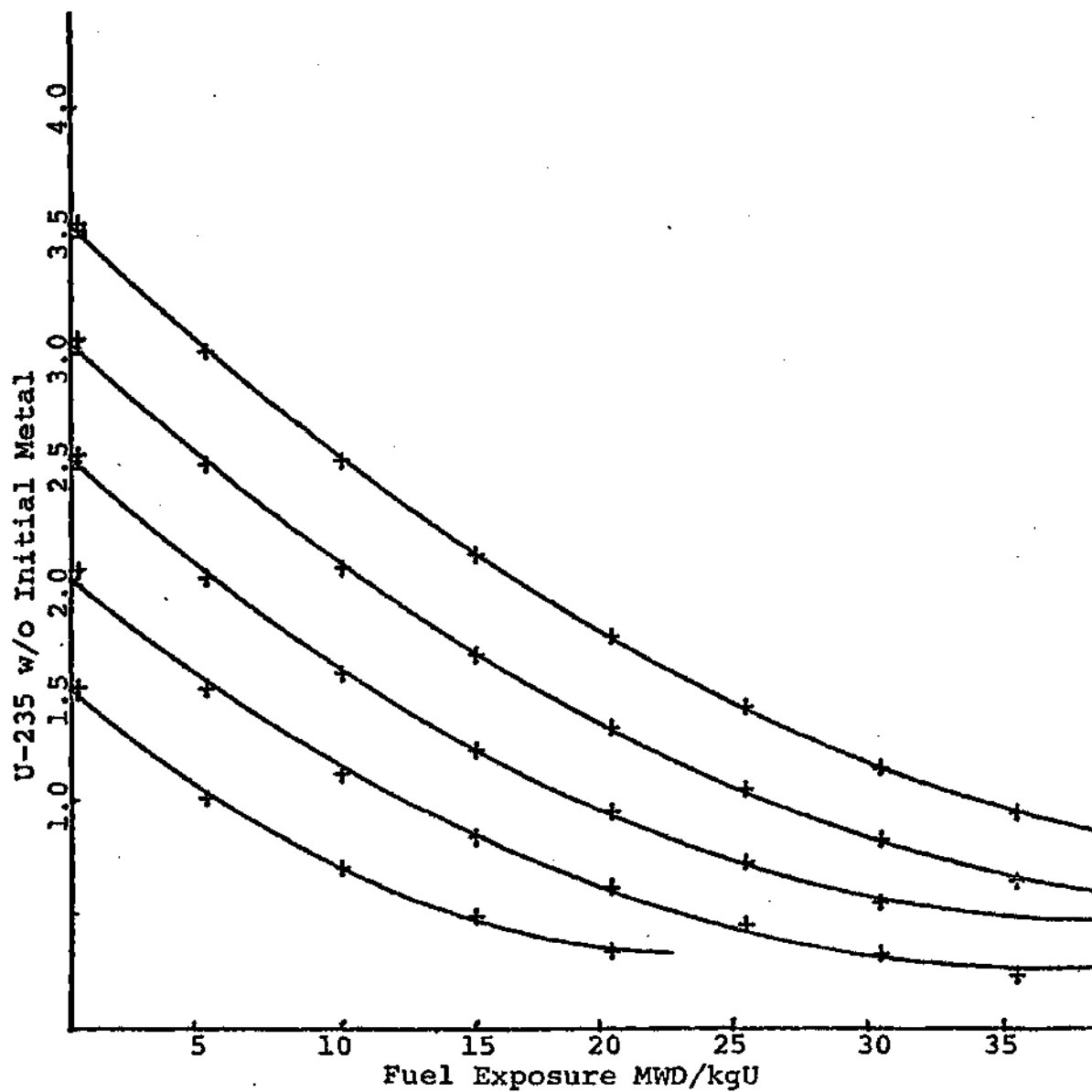


Figure 4. U-235 Enrichment as a Function of Initial Enrichment and Fuel Exposure

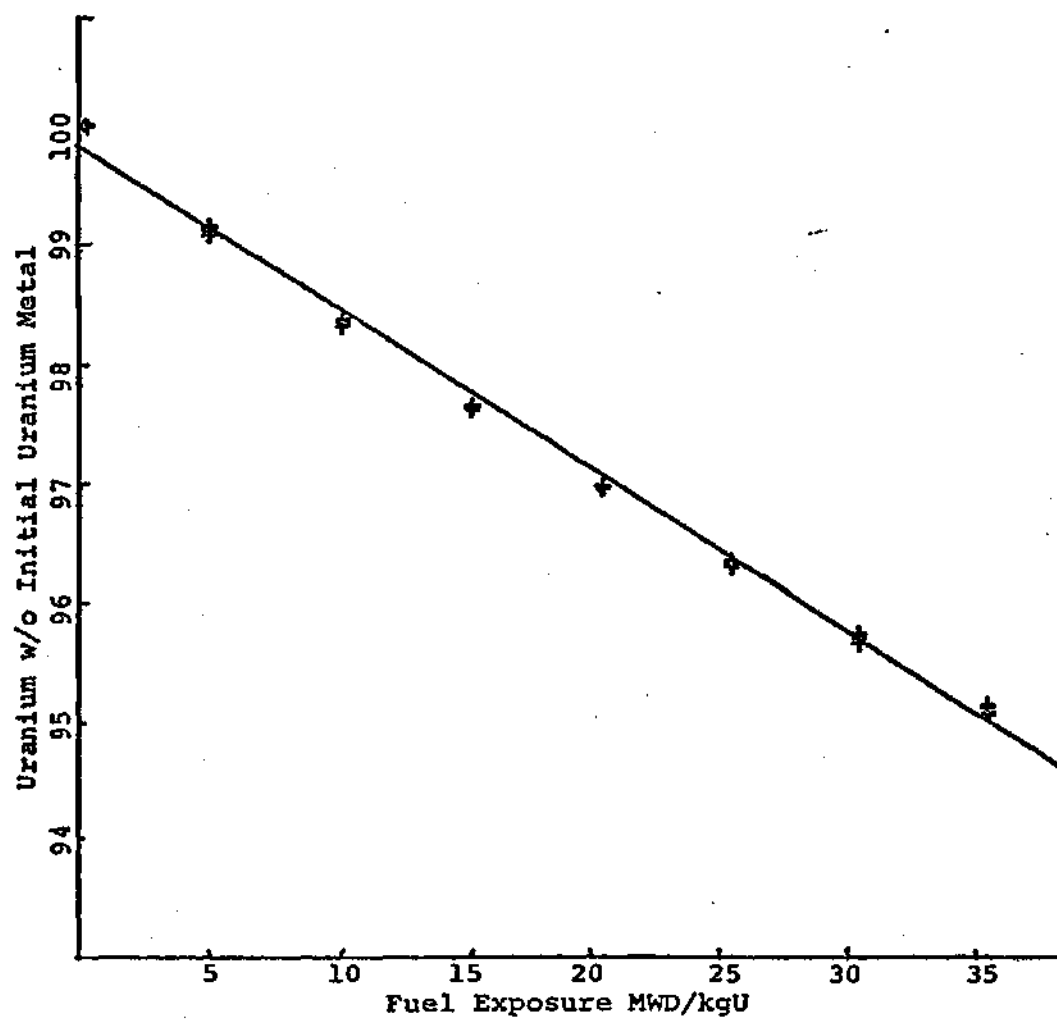


Figure 5. Uranium Weight as a Function of Fuel Exposure

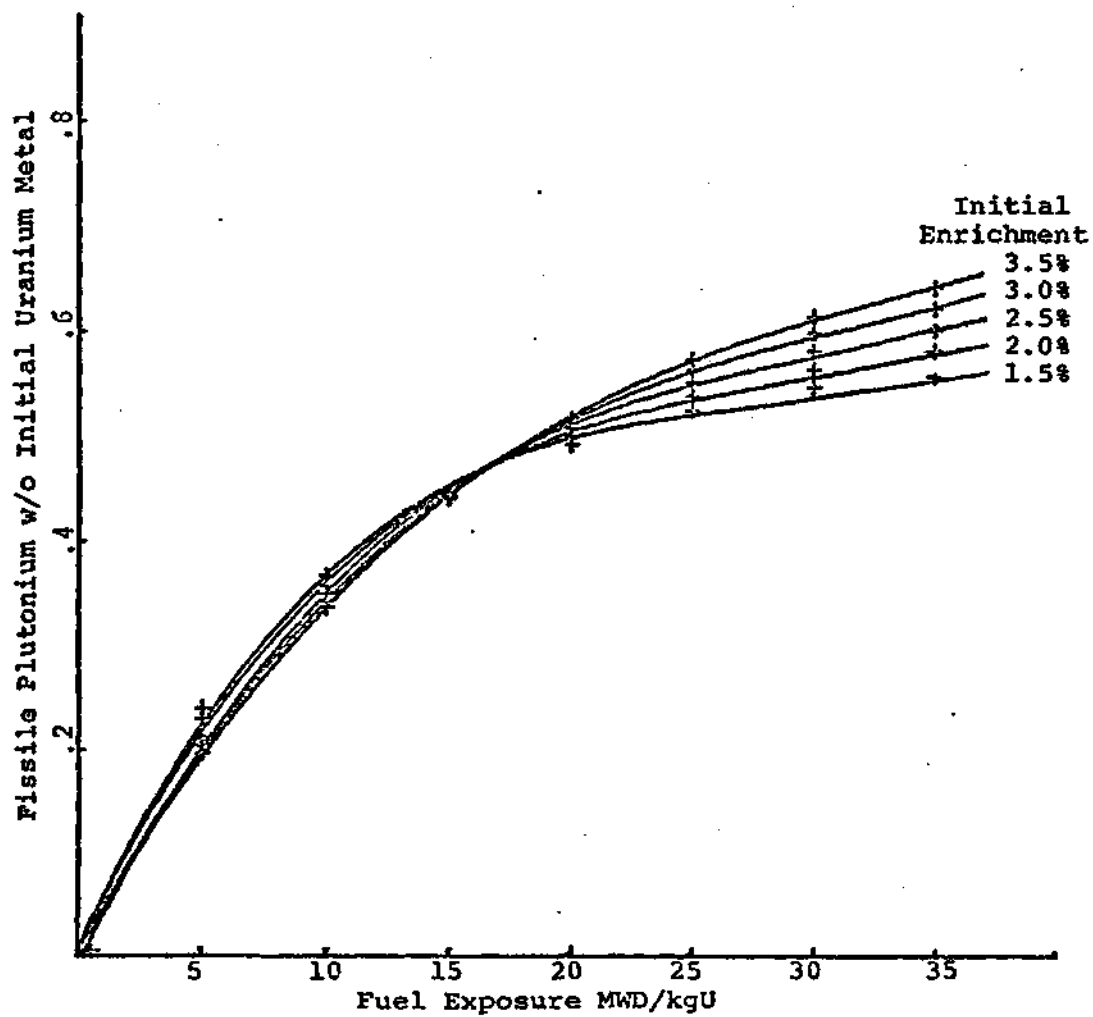


Figure 6. Fissile Plutonium Content as a Function of Initial Enrichment and Fuel Exposure

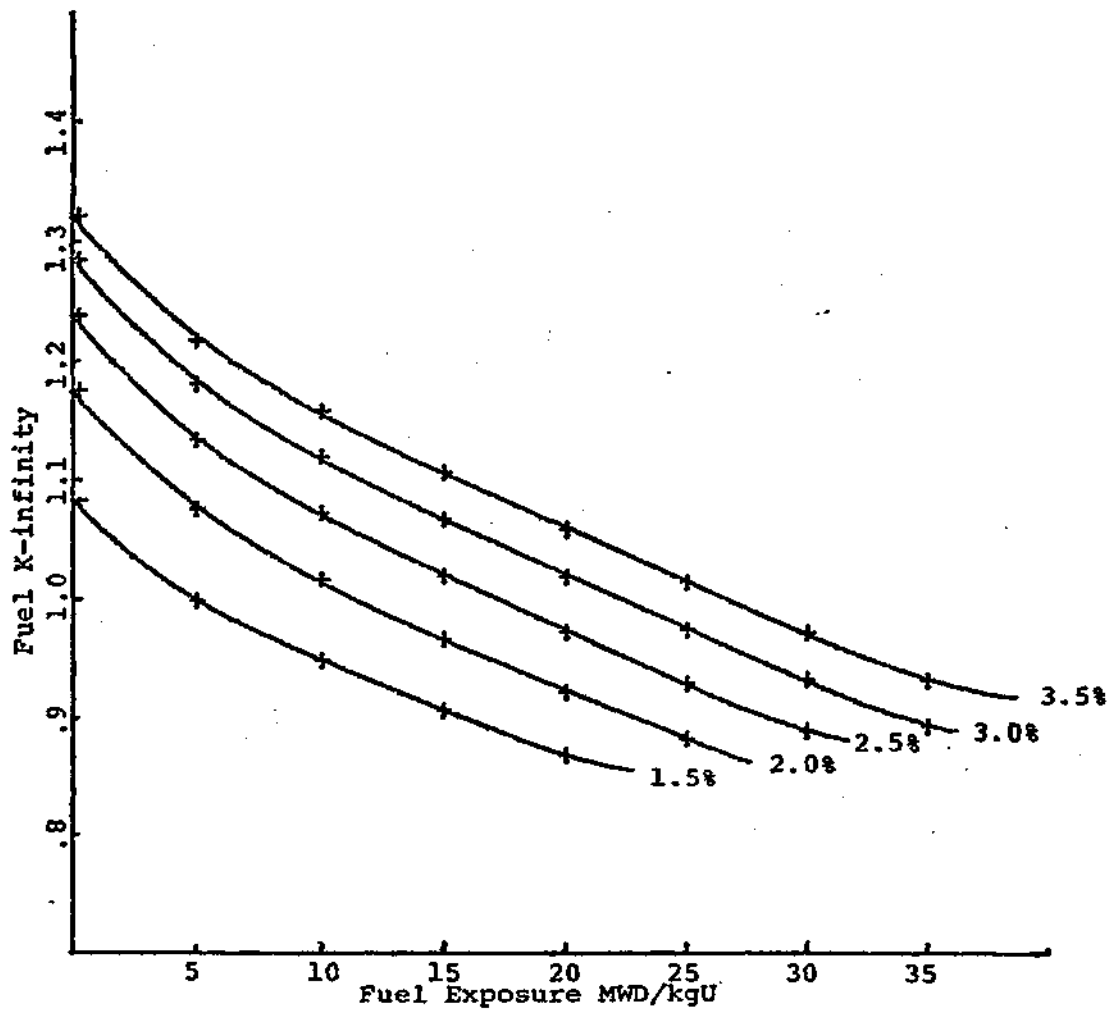


Figure 7. Fuel K-infinity as a Function of Initial Enrichment and Fuel Exposure

generated by the correlations.

Model

In this work, the foregoing assumptions and algorithms were developed into a computerized core simulator model. The basic flow of the computer program is shown in Figure 8. The main program, XPLOAD, reads run options and calls the five major subroutines. For cases without a coupled CINCAS calculation, the subroutine BATIN will read the following batch-related information:

1. Batch number,
2. Initial batch average enrichment,
3. Initial batch loading cycle,
4. Final batch discharge cycle,
5. First removal cycle for a reinserted fuel batch (optional),
6. Reinsertion cycle for a reinserted fuel batch (optional),
7. Core periphery fuel loading indicator, and
8. Equilibrium batch indicator.

This information is sufficient for the calculation of fuel exposures on a cycle-by-cycle, batch-by-batch basis. For cases in which fuel costs as calculated by CINCAS are desired the following additional information is also required for each fuel batch:

1. Fuel assembly initial weight in kilograms of contained Uranium and

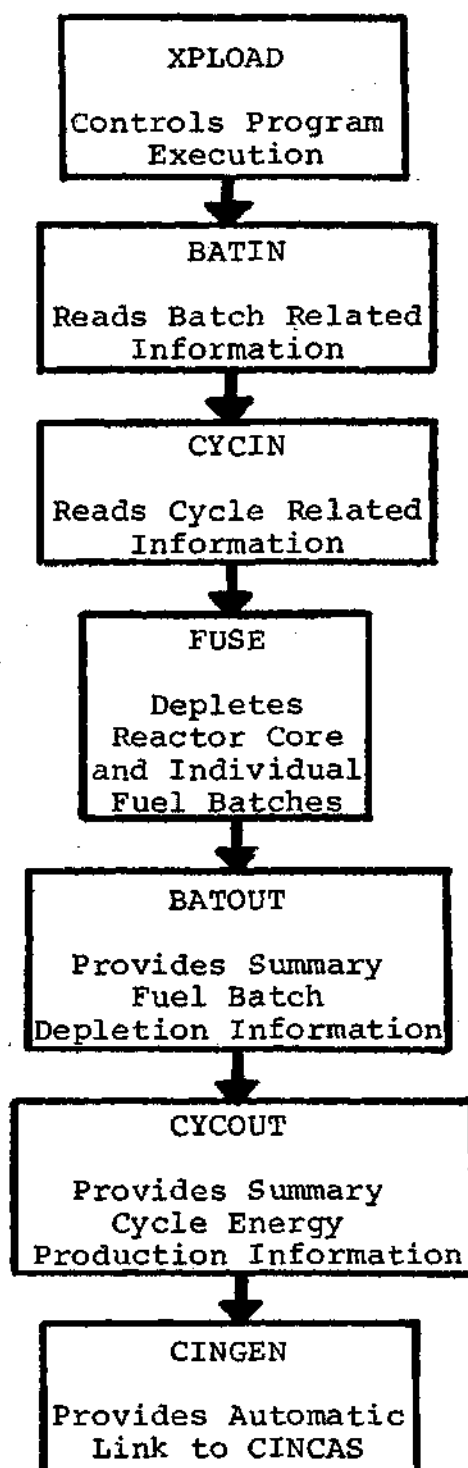


Figure 8. XPLOAD Flow Chart

2. Standard CINCAS input information excluding items calculated by XPLOAD.

The subroutine CYCIN reads the following cycle-related information for a case in which fuel costs will not be analyzed by CINCAS:

1. Cycle number,
2. End-of-cycle k-infinity, and
3. Equilibrium cycle indicator.

For cases which are to be analyzed using CINCAS, the following additional information is required for each cycle:

1. Thermal to electrical conversion efficiency,
2. Cycle startup date,
3. Cycle shutdown date, and
4. Equilibrium cycle length in months.

Based upon the input information, the subroutine FUSE depletes the reactor for each cycle. Utilizing the depletion algorithm, flow-charted in Figure 9, FUSE generates three arrays: BBURN, a two-dimensional array containing fuel assembly exposures for each batch on a cycle-by-cycle basis, BRNUP, a one-dimensional array containing batch fuel exposures at fuel discharge, and CORBU, a one-dimensional array containing core average exposures for each cycle in the study. These arrays are utilized in the subroutines BATOUT and CYCOUT to generate summary information regarding the fuel. BATOUT gives a fuel batch exposure summary based upon information contained in the BBURN and BRNUP arrays.

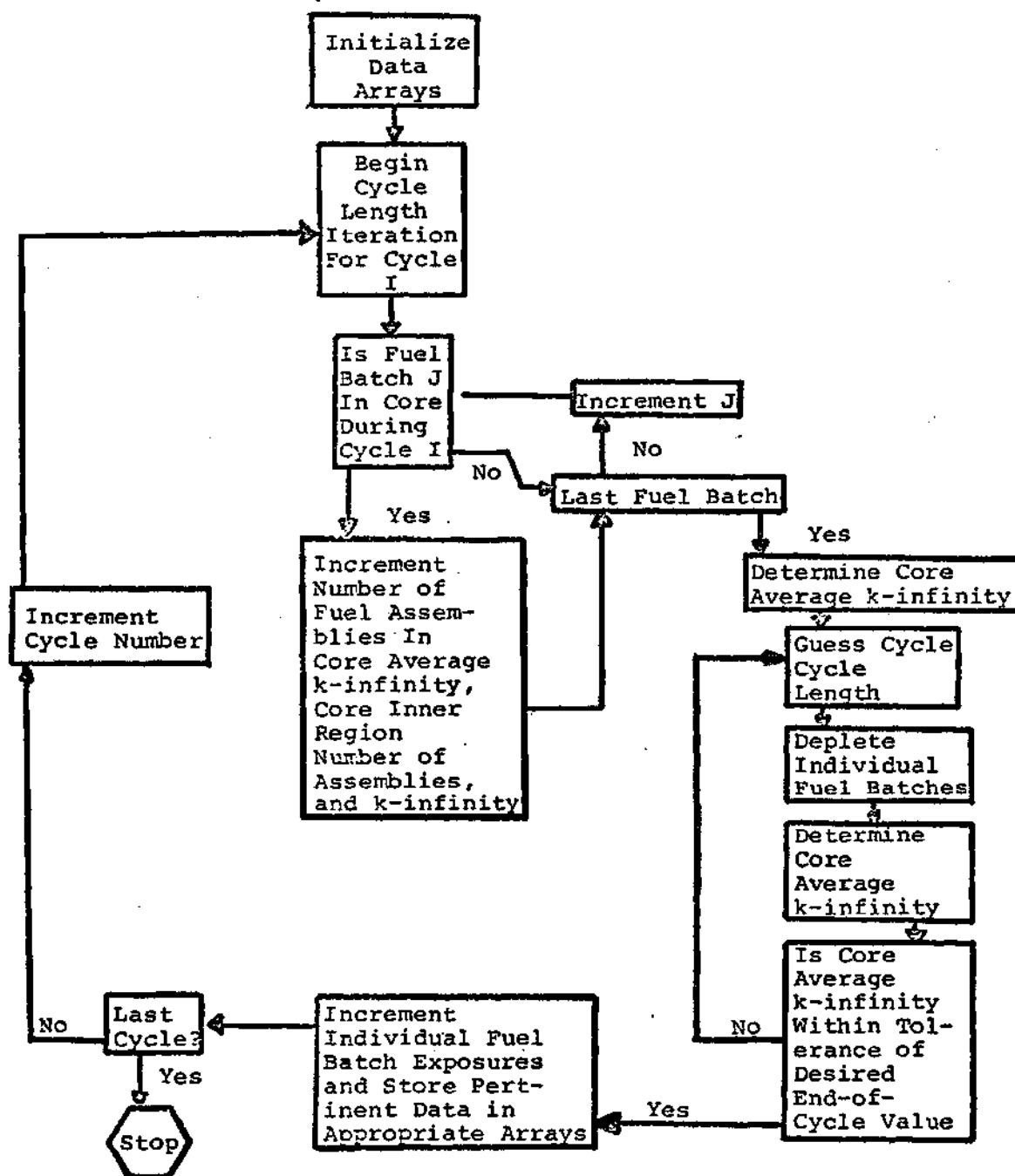


Figure 9. FUSE Logic

Tables 1 and 2 are the batch-related results of a sample problem. The heavy metal isotopic data represented in Table 1 was calculated from correlations developed using the results of LASER calculations. The output of CYCOUT for the same sample case is shown in Table 3.

For cases in which the analysis of fuel costs by CINCAS is desired, the subroutine CINGEN is called. This subroutine will read a standard set of CINCAS data cards and calculate batch fuel revenue requirements. These calculations require standard CINCAS input information with the exception of the following items which are calculated by XPLOAD:

1. Date card--withdrawal date, second insertion date, second withdrawal date,
2. Card type 4--all information (monthly energy production),
3. Card type 5--variable method of energy production,
4. Card type 7--all information (initial fuel enrichment and weight), and
5. Card type 8--all information (burnup-dependent data).

Table 1. XPLOAD Core Depletion Results

Batch No.	No. ASBL	U-235 w/o UI	Loading Cycle	Disch Cycle	Burnup MWD/MTU	U-235 w/o UF	URAN w/o MI	PU-FISS w/o MI	PU-TOT w/o MI
1	70	1.75	1	1	13651.	.760	97.937	.394	.539
2	70	2.45	1	2	25378.	.685	96.302	.546	.772
3	53	3.15	1	3	32810.	.820	95.266	.597	.862
4	17	2.70	2	3	24721.	.863	96.394	.548	.755
5	53	3.40	2	4	34186.	.921	95.075	.608	.875
6	17	2.70	3	4	25715.	.820	96.255	.555	.772
7	53	3.40	3	5	34823.	.900	94.986	.607	.881
8	17	2.70	4	5	25528.	.828	96.281	.554	.769
9	53	3.40	4	6	34716.	.903	95.001	.607	.880
10	17	2.70	5	6	25471.	.830	96.289	.553	.768
11	53	3.40	5	7	34661.	.905	95.008	.607	.879
12	17	2.70	6	7	25535.	.828	96.280	.554	.769
13	53	3.40	6	8	34708.	.903	95.002	.607	.880
14	17	2.70	7	8	25511.	.829	96.284	.554	.769
15	53	3.40	7	8	23336.	1.428	96.587	.551	.719
16	17	2.70	8	8	13841.	1.487	97.911	.394	.503
17	53	3.40	8	8	10647.	2.351	98.356	.325	.393

Table 2. XPLOAD Batchwise Cycle-by-Cycle Burnups

Load Cycle	Batch				Discharge Exposure	Discharge Cycle
1	1	13651.	0.	0.	13651.	1
1	2	14936.	10442.	0.	25378.	2
1	3	9718.	11650.	11442.	32810.	3
2	4	12809.	11912.	0.	24721.	3
2	5	9765.	12934.	11487.	34186.	4
3	6	13992.	11723.	0.	25715.	4
3	7	10801.	12747.	11275.	34823.	5
4	8	13927.	11600.	0.	25528.	5
4	9	10727.	12615.	11373.	34716.	6
5	10	13773.	11697.	0.	25471.	6
5	11	10585.	12719.	11358.	34661.	7
6	12	13868.	11667.	0.	25535.	7
6	13	10671.	12687.	11349.	34708.	8
7	14	13844.	11666.	0.	25511.	8
7	15	10650.	12686.	0.	23336.	8
8	16	13841.	0.	0.	13841.	8
8	17	10647.	0.	0.	10647.	8

Table 3. XPLOAD Cycle Length Predictions

Cycle No.	Cycle Length MWD/MTU
1	13037.
2	10796.
3	11942.
4	11860.
5	11702.
6	11798.
7	11775.
8	11771.

CHAPTER IV

FUEL FAILURES-FUEL COSTS--A PARAMETRIC ANALYSIS

The premature replacement of fuel is an alternative available to operating nuclear power plants to extend cycle lengths, utilize excess material being carried in inventory, or to replace fuel assemblies which have experienced cladding failure. To date, mainly due to poor fuel performance, over half of the operating nuclear power plants have been forced to replace fuel prematurely. Early fuel replacement results in a perturbation to long-range refueling plans. To determine the effects of early fuel discharges on fuel cycle energy production and fuel cycle costs, a parametric analysis was performed using the core simulator model coupled with CINCAS to calculate fuel cycle costs.

The fuel cycle plan for the SNUPPS reactor utilized in this analysis had a fuel loading comprised of 193 fuel assemblies. The first core consisted of 70 fuel assemblies with an average enrichment of 1.75% U-235, 70 fuel assemblies with an enrichment of 2.45%, and 53 assemblies with an enrichment of 3.15%.

Fuel for each of the reloads was separated into two batches: a high enrichment batch consisting of 53 assemblies with an enrichment of 3.4% and a low enrichment batch

consisting of 17 fuel assemblies with an enrichment of 2.7%. The 3.4% enriched fuel had a design nuclear life of three cycles at full power, and the 2.7% enriched fuel had a design life of two cycles. This resulted in the basic refueling scheme shown in Table 4.

For analysis by the core simulator, an equilibrium cycle refueling was perturbed by prematurely discharging fuel assemblies and replacing them with fresh fuel. This replacement of prematurely discharged fuel was based on the following rules:

1. Only fuel of 3.4% and 2.7% enrichments were available for replacement of the prematurely discharged fuel.
2. The fresh fuel which was inserted in place of the premature discharge would remain in core for its "design nuclear life." Thus 3.4% fuel would remain in core for three full cycles and 2.7% enriched fuel would remain in core for two cycles.
3. The refueling scheme should be devised consistent with rules one and two such that a minimum perturbation of future reloading plans would occur.

Rule 1 is plausible from several aspects. First, the detailed nuclear analysis of the reload core will be much simpler if cross-sections are not required for another initial enrichment fuel assembly. Second, keeping the number of reload fuel assembly enrichment to a minimum will

Table 4. SNUPPS Reactor Fuel Cycle Plan

Batch Number	Number of Assemblies	Initial Enrichment	Loading Cycle	Discharge Cycle
1	70	1.75	1	1
2	70	2.45	1	2
3	53	3.15	1	3
4	17	2.70	2	3
5	53	3.40	2	4
6	17	2.70	3	4
7	53	3.40	3	5
8	17	2.70	4	5
9	53	3.40	4	6
10	17	2.70	5	6
11	53	2.70	5	7

Table 5. Representative Refueling Patterns Investigated

Batch	Enrich	-----Number of Assemblies-----				Loading Cycle	Discharge Cycle
		Base Case	Case 4 [*]	Case 8 ^{**}	Case 12 ^{***}		
8A	2.7	17	<u>5</u>	17	17	4	5
8B	2.7	0	<u>12</u>	0	0	4	4
9A	3.4	53	53	<u>41</u>	<u>41</u>	4	6
9B	3.4	0	0	<u>12</u>	0	4	4
9C	3.4	0	0	0	<u>12</u>	4	5
10	2.7	17	17	<u>29</u>	17	5	6
11	3.4	53	<u>65</u>	53	53	5	7
12	2.7	17	17	17	17	6	7
13	3.4	53	53	53	<u>65</u>	6	8
14	2.7	17	17	17	<u>5</u>	7	8
15	3.4	53	53	53	53	7	9
16	2.7	17	17	17	17	8	9
17	3.4	53	53	53	53	8	10

* 12--2.7% ASBL (Batch 8B) are replaced by 12--3.4% ASBL (added to Batch 11)

** 12--3.4% ASBL (Batch 9B) are replaced by 12--2.7% ASBL (added to Batch 10)

*** 12--3.4% ASBL (Batch 9C) are replaced by 12--3.4% ASBL (added to Batch 13).
This results in 12 less 2.7% ASBL loaded in Batch 14.

ease the problems associated with the actual fuel loading procedure at the reactor site. Third, utilizing the same enrichment as existing reload fuel is also practical from a procurement aspect. If it were necessary to locate licensable fuel on short notice, the best source of reload fuel would be another SNUPPS reactor utilizing a similar refueling plan.

Rule 2 is based upon the economical utilization of the reload fuel. Once the fuel is inserted into the reactor, minimum overall energy costs require extracting near the equilibrium cycle energy from the fuel.

Rule 3 is brought about by long-term procurement practices. Current trends in the nuclear industry call for the letting of contracts eight to ten years in advance of the start of energy production from a nuclear power plant. Since this material is scheduled for delivery based on an unperturbed schedule of operation, a quick return to equilibrium refueling conditions will minimize inventories of material.

Using these three rules, perturbations to reactor refueling following the attainment of an equilibrium cycle condition were considered. The perturbations considered consisted of the discharge of from one to twelve low enrichment fuel assemblies after one cycle of operation; the discharge of from one to sixteen high enrichment assemblies after one cycle of operation; and the discharge of

from one to sixteen high enrichment assemblies after two cycles of operation.

For the cases in which the 2.7% enriched fuel assembly was replaced with a 3.4% assembly after one cycle of operation major fluctuations in cycle energy production were apparent for the first two cycles as shown in Figure 10. The increase in the first perturbed cycle's energy production was due to the higher initial core reactivity because of the reactivity difference between the once-burned 2.7% fuel and the fresh 3.4% fuel. The increase in cycle energy production brought about a corresponding increase in fuel batch end-of-cycle exposures which resulted in a decrease in reactivity for the fuel which remained in core for the next cycle of operation. In addition to this effect, the fresh 2.7% fuel which was originally scheduled for loading at the beginning of the second cycle following the perturbed discharge was displaced by the less reactive once-burned 3.4% enriched fuel. The net result is a core loading for the second cycle which had significantly less initial reactivity than that contained in the equilibrium cycle core. After variations in the first two perturbed cycles' energy production, the fuel cycle length returned to within 4% of the equilibrium fuel cycle value for up to twelve assemblies prematurely discharged.

The variation of cycle energy with the number of low enrichment fuel assemblies which were discharged

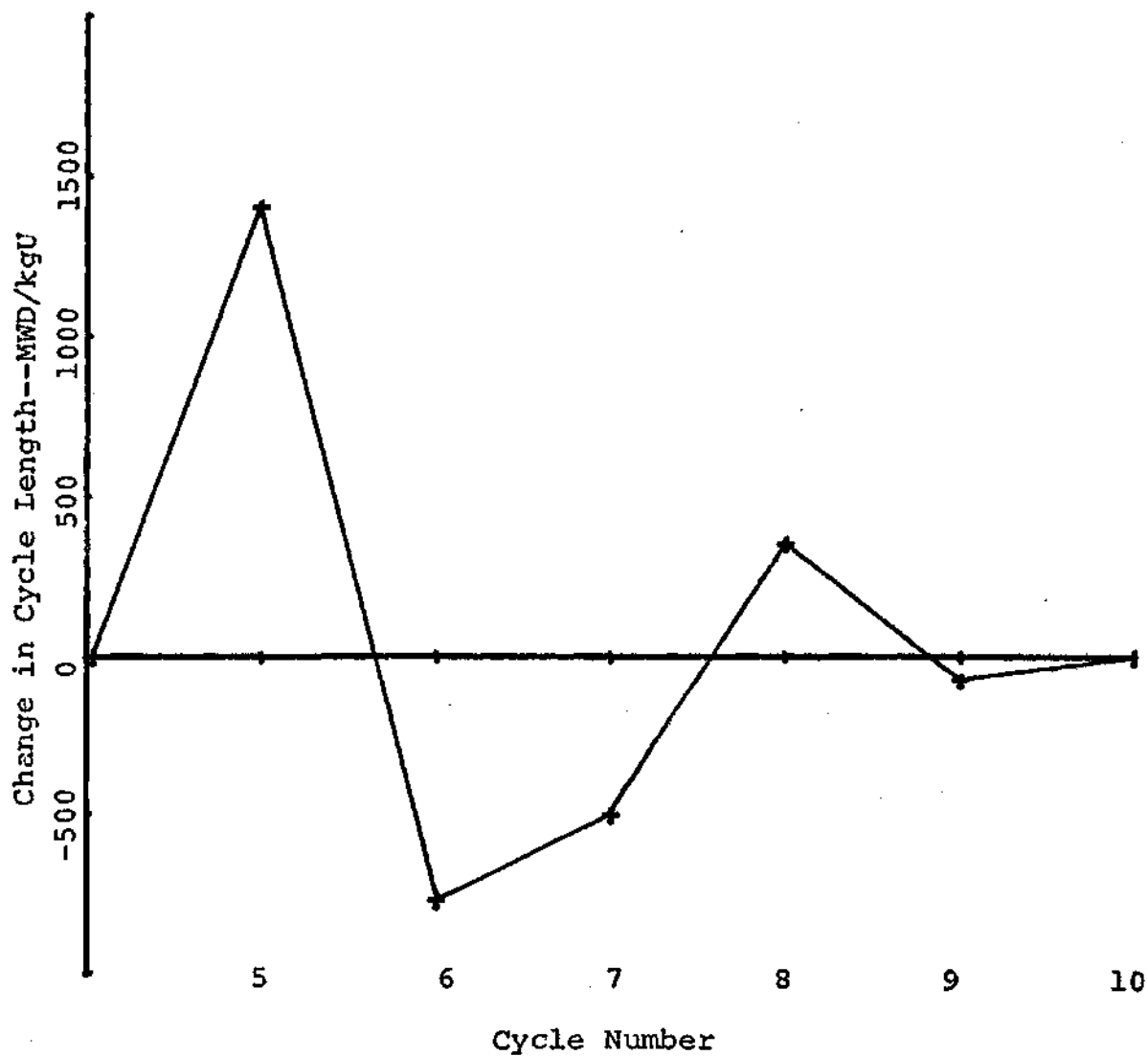


Figure 10. The Effect of the Early Discharge of Twelve Low Enrichment One-Cycle Fuel Assemblies on Cycle Energy Production

prematurely is shown in Figure 11. It is interesting to note the linear relationship between the number of assemblies in the discharge batch and cycle energy production. This linearity was the result of the linear relationships used for cycle length predictions in the core simulator model, the linear model which is used to allocate fuel batch burnups, and the linear nature of the correlated values of k -infinity over the range of discharge exposures under examination.

In spite of major fluctuations in cycle-by-cycle energy production in the five cycles immediately following the abnormal refueling, the total energy produced in the perturbed case varied from the energy produced in the unperturbed case by only 323 MWD/MTU or .5% of the energy produced in the five cycles following the early fuel discharge when 12 fuel assemblies were replaced after one cycle of operation.

For the cases in which the 3.4% enriched fuel assemblies were replaced with 2.7% enriched fuel, the fuel cycle energy fluctuations resulted from a mechanism similar to that which caused the fluctuations in the previous case. However, in these instances, the reactivity difference between the once-burned 3.4% fuel assemblies and the fresh 2.7% fuel was much less, and hence the fluctuations in cycle energy production were much less than those which were observed under the previous discharge conditions. Another benefit of the small reactivity difference between the reload

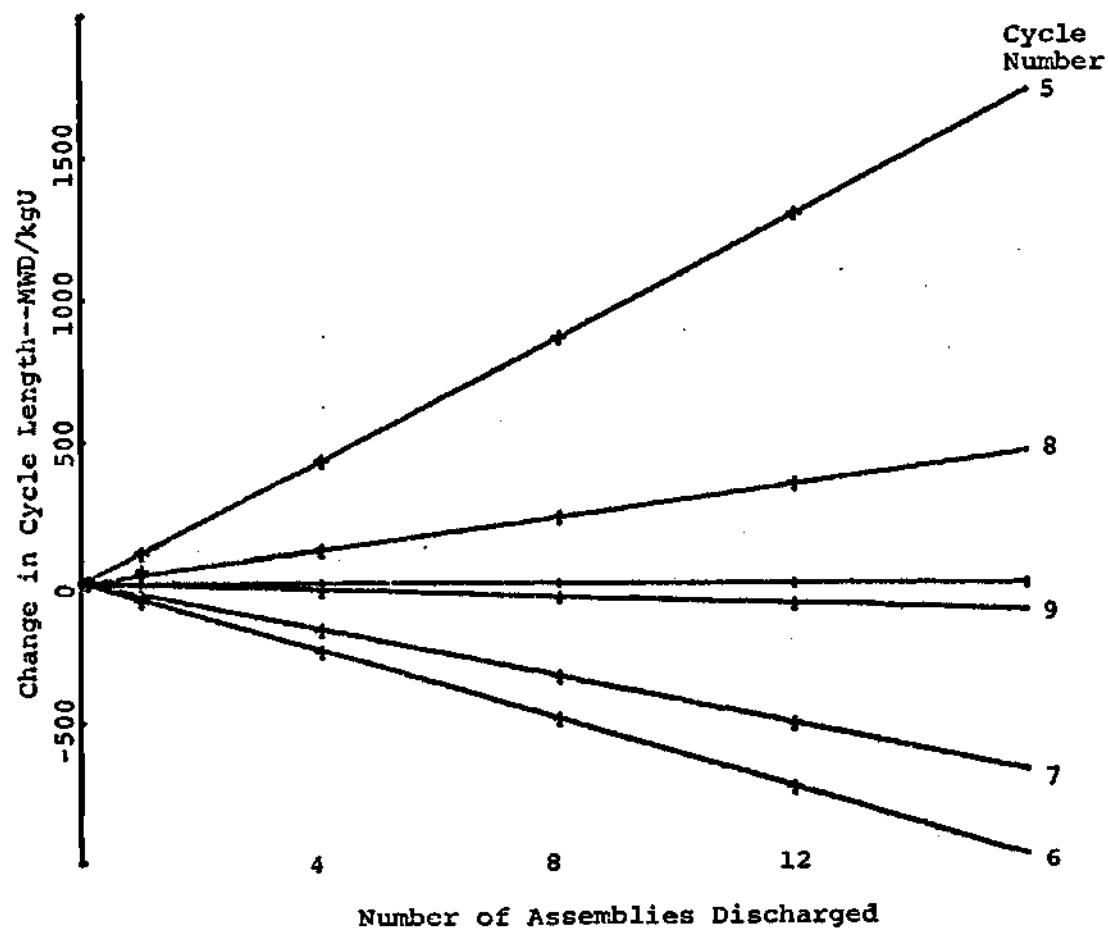


Figure 11. The Effect of Early Discharge Batch Size on Subsequent Fuel Cycle Lengths for the Early Replacement of One-Cycle Low Enrichment Fuel Assemblies

fuel and the discharged fuel was a quick return to equilibrium cycle as shown in Figure 12. Figure 13 shows the effect of the size of the perturbed batch on future cycle energy production. It is apparent that major fluctuation in cycle energy production occurs in the initially perturbed cycle. As in the previous case, the total variation in cycle energy production following the perturbation was relatively small. In this case, the total variation in cycle energy over the five year period following the refueling perturbation was only 0.4% of the total energy production in this period for the early discharge of twelve fuel assemblies.

Cycle energy fluctuations were greatest for the replacement of high enrichment fuel assemblies after two cycles of irradiation. This effect is explained by the large reactivity difference in the discharged assemblies and the fresh fuel which serves as its replacement. With the exception of the larger reactivity difference, the replacement of the twice-burned high enrichment fuel was similar to the previously analyzed replacement of the low enrichment fuel. Figures 14 and 15 show the effects of early fuel replacement on cycle energy production and the size of the prematurely discharged fuel batch on the magnitude of the cycle energy fluctuations. The cause of the energy fluctuations was the same as in the case of the early replacement of the low enrichment fuel. The cycle immediately following the reload perturbation had excess reactivity which resulted in a longer

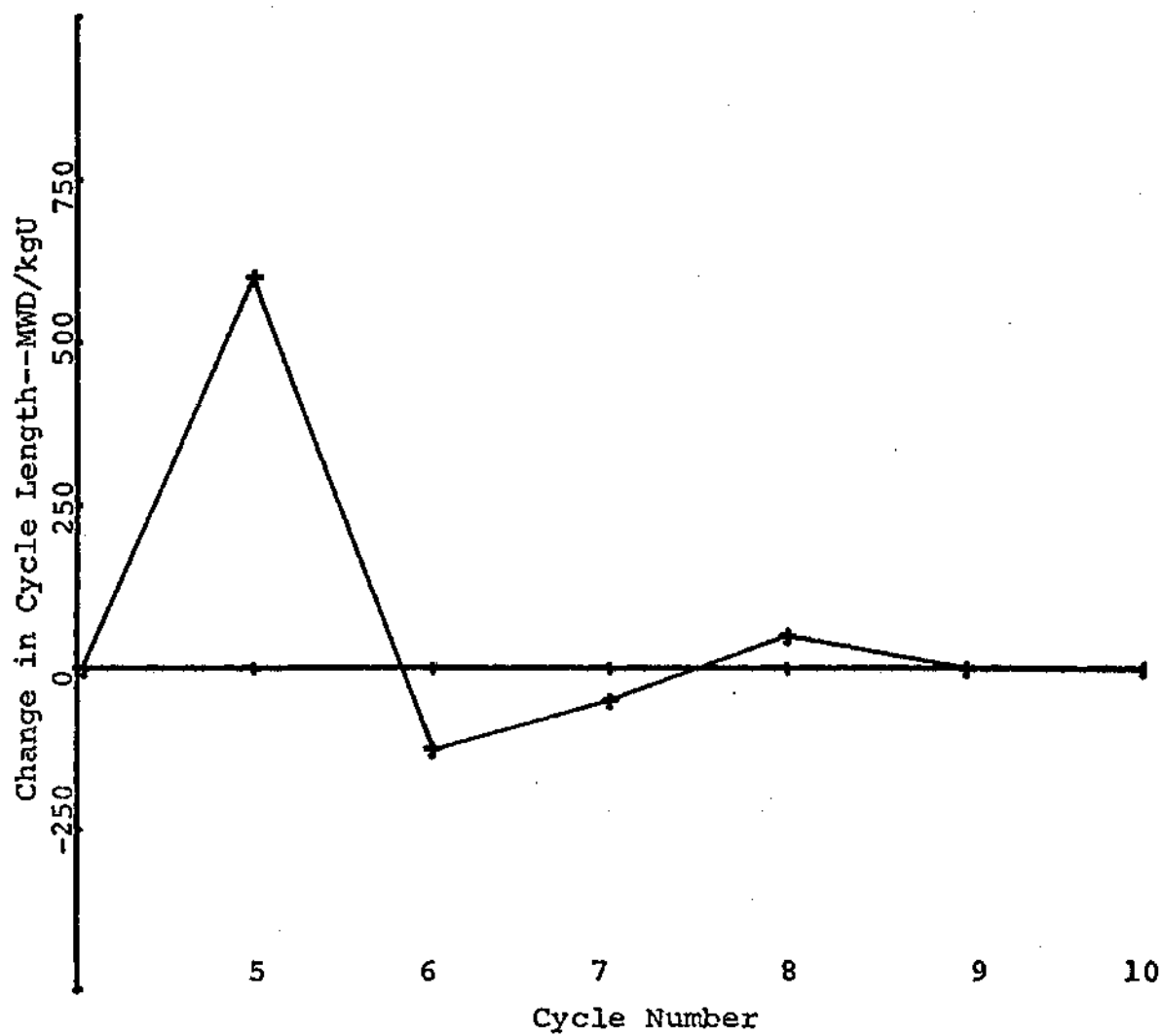


Figure 12. The Effect of the Early Discharge of Twelve High Enrichment One-Cycle Fuel Assemblies on Cycle Energy Production

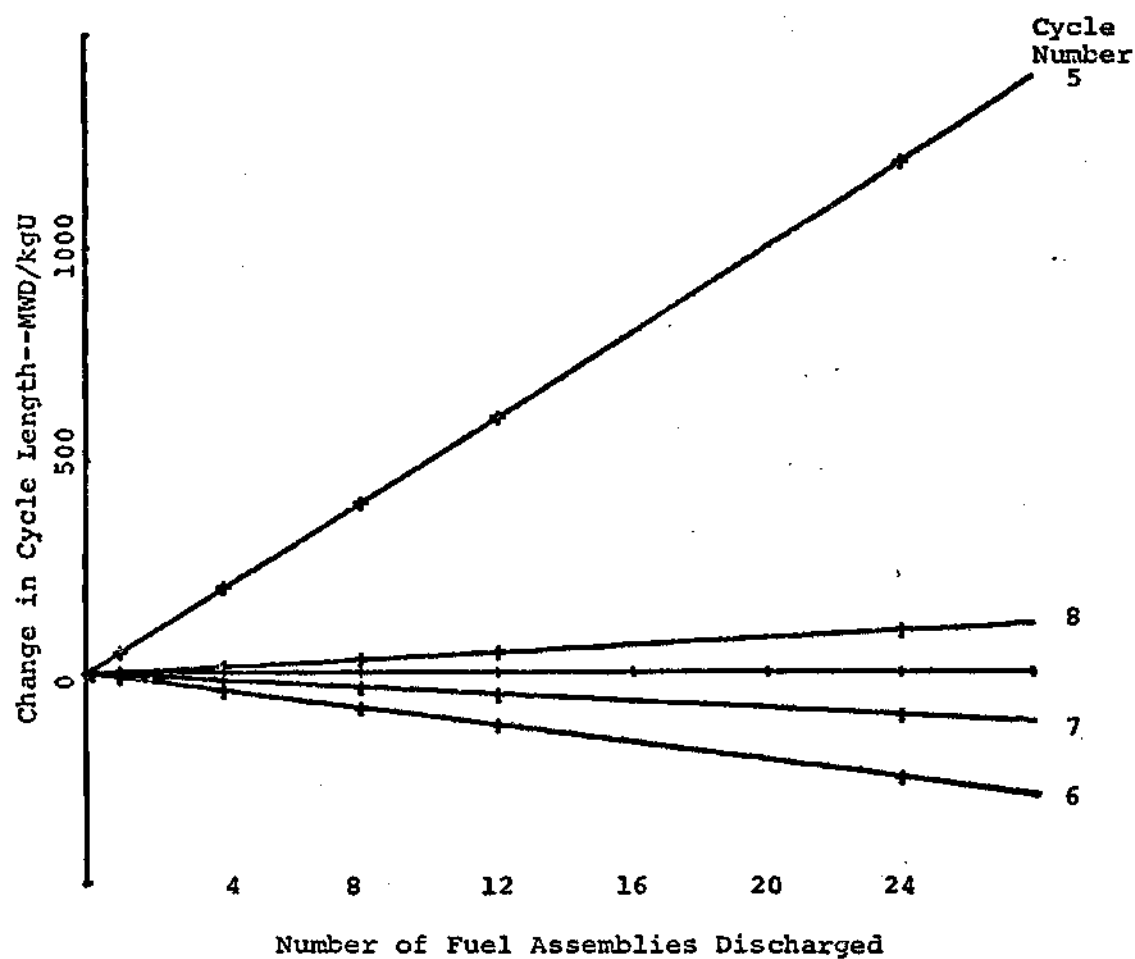


Figure 13. The Effect of Early Discharge Batch Size on Subsequent Fuel Cycle Lengths for the Early Replacement of One-Cycle High Enrichment Fuel Assemblies

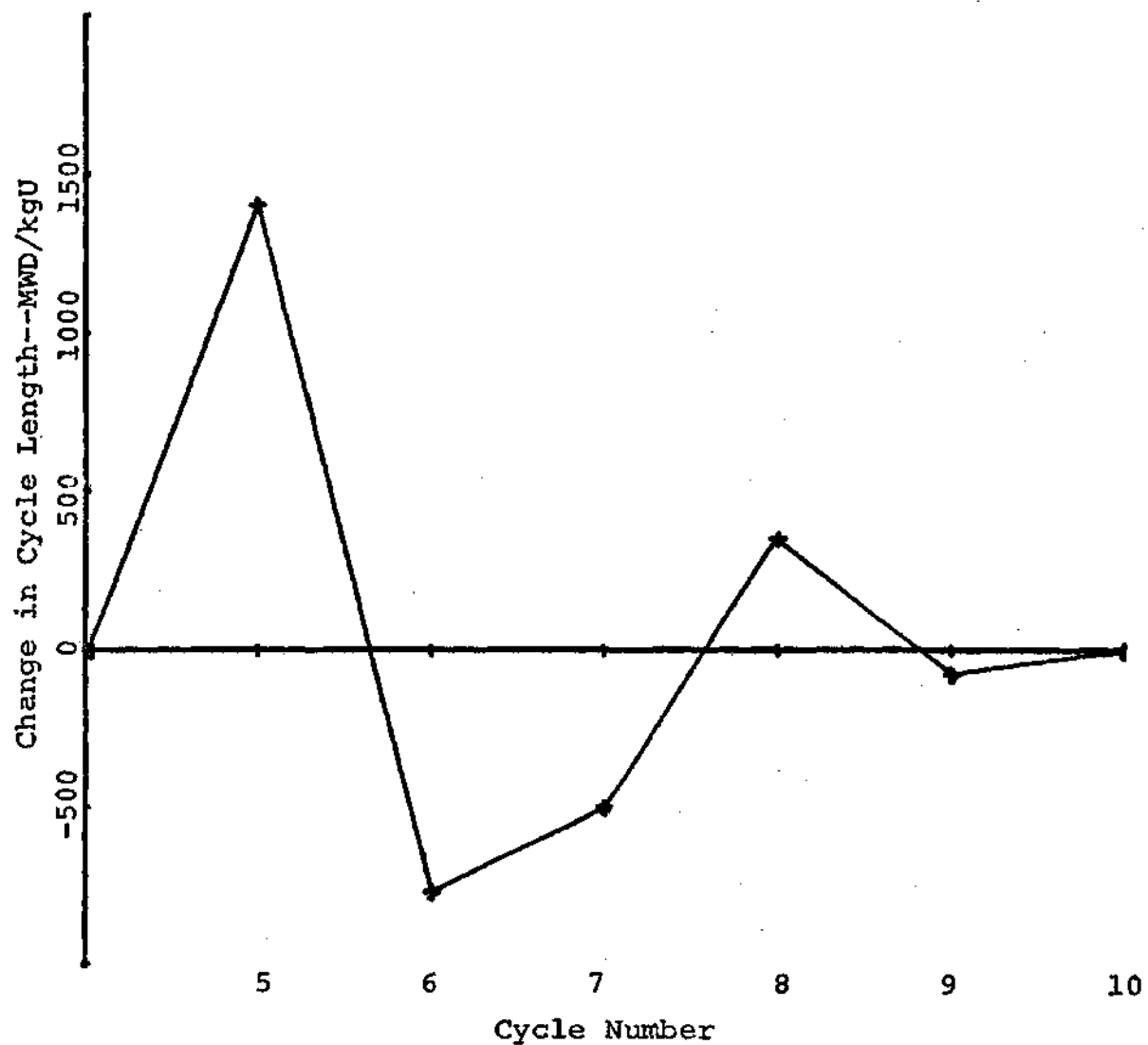


Figure 14. The Effect of the Early Discharge of Twelve High Enrichment Two-Cycle Fuel Assemblies on Cycle Energy Production

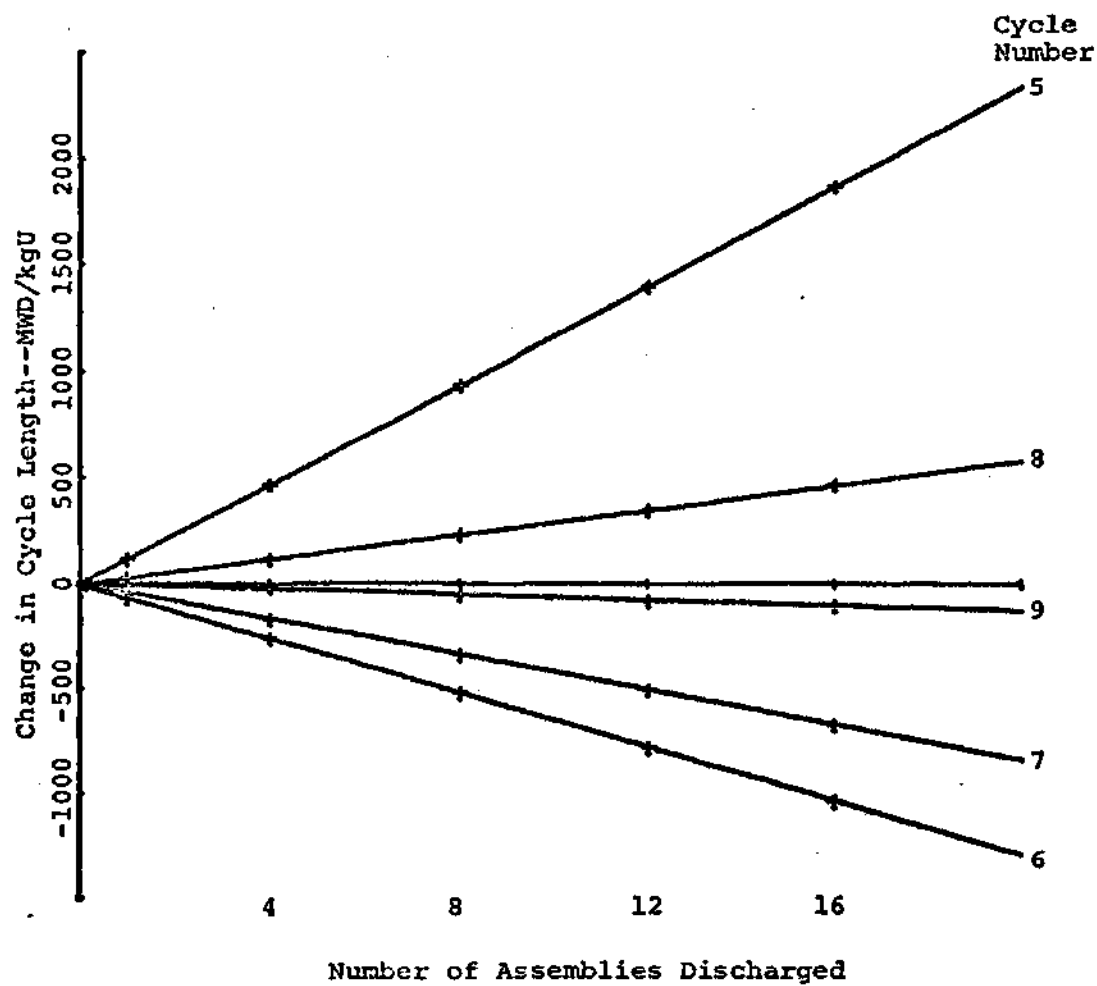


Figure 15. The Effect of Early Discharge Batch Size on Subsequent Fuel Cycle Lengths for the Early Replacement of High Enrichment Fuel After Two Cycles of Irradiation

cycle. The subsequent cycle utilized once-burned 3.4% fuel assemblies in lieu of the scheduled 2.7% fuel. This, coupled with the higher exposure of the fuel remaining in the core resulted in a drop in the beginning-of-cycle reactivity. The effect of the non-equilibrium reload had disappeared for all practical purposes after the second fuel cycle following the perturbed reload. The net effect on cycle energy production for the five cycles immediately following the premature discharge was a net increase of less than .7% in total energy production for up to twelve fuel assemblies discharged prematurely.

The fluctuations in cycle energy production produced corresponding changes in batchwise energy production. Because of the oscillating nature of the cycle energies after the reload perturbation, the overall effect on fuel batch discharge burnup was relatively small. The largest changes in batch discharge exposures occurred for fuel which was discharged at the end of the first perturbed cycle. In these instances, the fuel assemblies were driven to higher exposures because of the increased fuel cycle lengths. Increased core energy production resulted in increases in fuel discharge exposures of 5.4% and 5.0% for the cases involving the replacement of twelve high enrichment fuel assemblies after two cycles and twelve low enrichment assemblies after one cycle of irradiation respectively. The early replacement of twelve high enrichment assemblies after

one cycle of irradiation resulted in a maximum increase of 2.7% in the batch discharge exposure. The forecasted batch discharge exposures for fuel in subsequent cycles was also sensitive to cycle energy fluctuations. In the cases of replacement of high enrichment fuel after two cycles and low enrichment fuel after one cycle, these cycle energy fluctuations resulted in variations in batch discharge exposures. This effect was most pronounced for fuel which was in core for shorter periods of time (i.e. the low initial enrichment fuel).

Analyses of batch fuel costs using projected 1980 cost data and CINCAS showed that the early replacement of fuel resulted in significant increases in fuel costs over a ten year time period. This cost can be thought of as resulting from two components; the first being the cost of the fuel which was discharged prematurely, and the second the cost of the makeup fuel. Previous analyses with CINCAS had shown an increase in batch fuel costs with increasing fuel assembly exposure. This variation is depicted in Figure 16. Since the variation from the base case for fuel discharge exposures was relatively small, the variation in individual batch energy costs was also small. The early fuel discharge batches will have slightly lower net fuel costs because of lower exposures at discharge. This lowering of batch fuel costs is offset by an increase in fuel costs caused by the fuel which is required to replace the fuel that is discharged

Table 6. Projected Cost Data Used in CINCAS Analyses

Component Costs

Ore Cost--\$/lb U_3O_8	\$ 20.00
Conversion Cost--\$/lbU as UF_6	1.80
Unit separative work costs--\$/kgSWU	100.00
Fabrication costs--\$/kgU	120.00
Spent fuel storage and shipping costs--\$/kgU	10.00
Reprocessing cost--including reconversion--\$/kgU	120.00
Plutonium value--\$/g fissile	16.00

Overages

U_3O_8 to UF_6 conversion loss--%	1.0
Fabrication overage--%	1.5
Uranium reprocessing loss--%	1.5
Plutonium reprocessing loss--%	1.5
Enrichment plant tails--%	.3

Lead Times

U_3O_8 Payment lead time--months	18
UF_6 Payment lead time--months	14
Enrichment payment lead time--months	12
Fabrication payment lead time--months	0
Reprocessing--months after shutdown	5
Sale of plutonium--months after reprocessing	7
Annual Income Tax Rate, %	50
Fuel and working capital carrying charge rate %	16

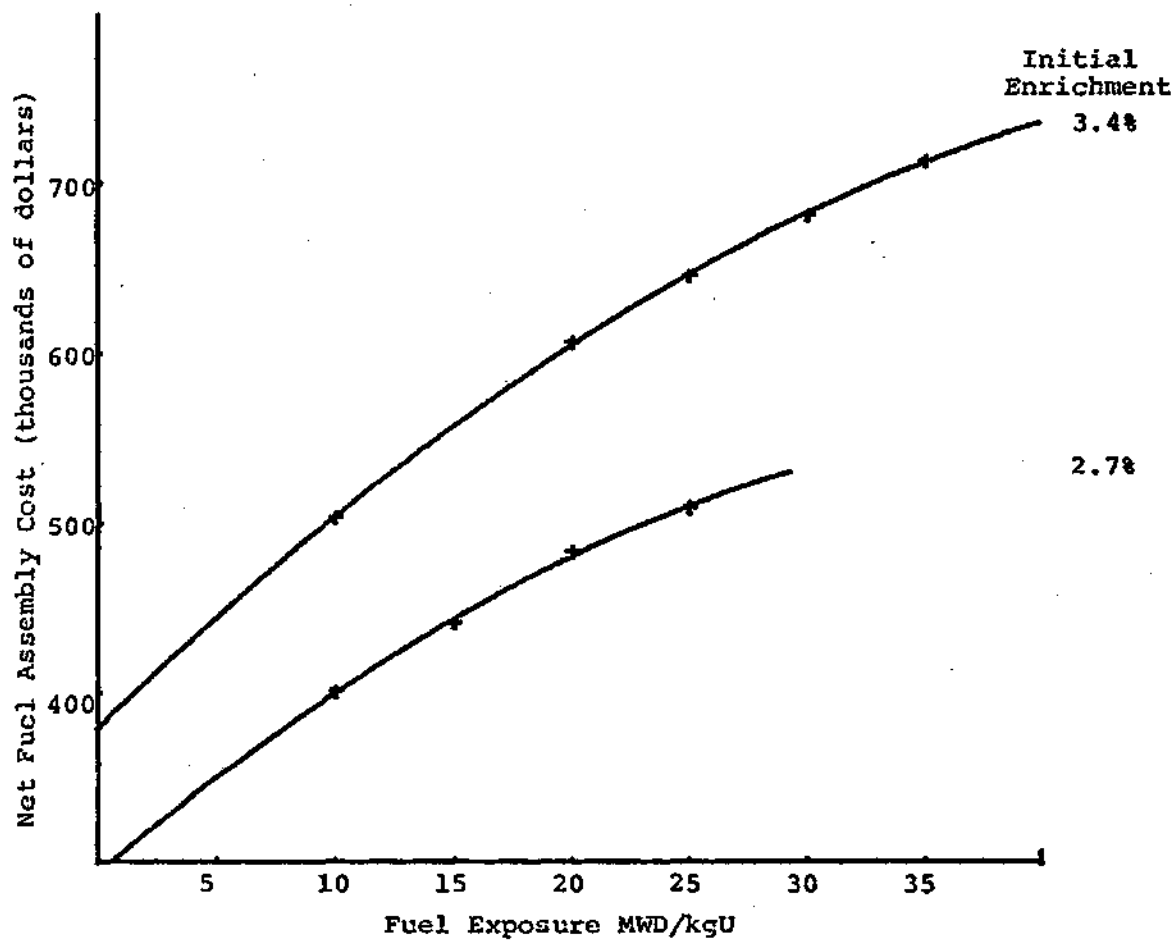


Figure 16. The Effect of Fuel Exposure on Net Fuel Assembly Cost

prematurely. In all cases under study, the net result of early fuel discharge was an increase in overall case fuel costs.

The predicted effect of the size of the prematurely discharged fuel batch on case fuel costs is shown in Figure 17. The effect of early discharges on total fuel costs is greatest when the smallest percentage of the fuel design life is achieved, while the achievement of a higher percentage of the fuel design life results in substantially lower overall fuel costs. This effect is tied to the energy-independent quantities of fuel cost such as fabrication, fuel shipping, and reprocessing. These costs are computed on a dollars per unit mass basis and therefore the cost of the service is not dependent upon energy extraction. By extracting the greatest amount of energy from a given fuel assembly, the contribution of the energy-independent quantities to the total cost is minimized.

Fuel cycle energy costs calculated by CINCAS showed large variations in cycle energy costs for the perturbed fuel loadings. The results of these calculations are shown in Figure 18. For Case 4, the energy cost fluctuation is primarily due to increased fabrication and reprocessing costs on a per kwhr basis for the discharged fuel. These costs are partially offset by a 12% increase in cycle energy output for the cycle where the peak fuel costs occur. The subsequent drop in fuel costs below the base case fuel costs

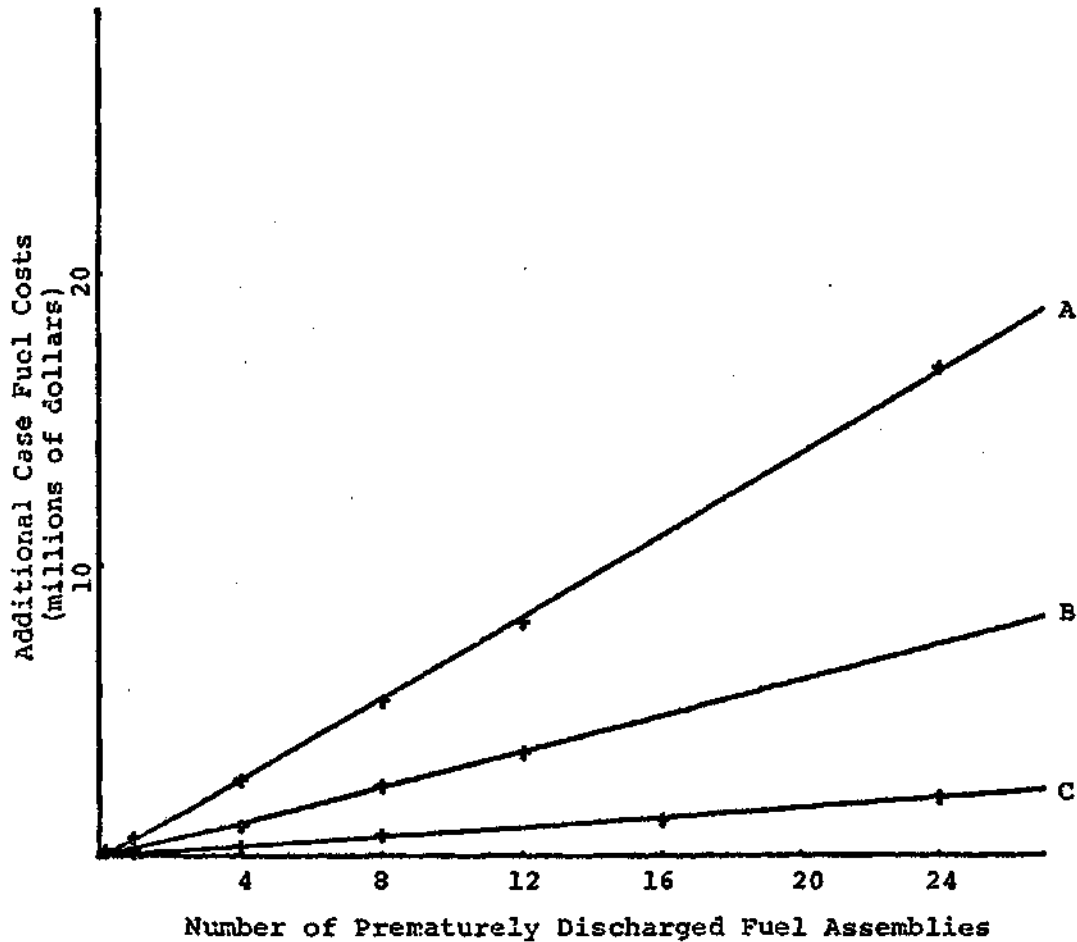


Figure 17. The Effect of Premature Fuel Discharge Batch Size on Case Fuel Costs
(A) High enrichment fuel discharged after one cycle; (B) Low enrichment fuel discharged after one cycle; (C) High enrichment fuel discharged after two cycles

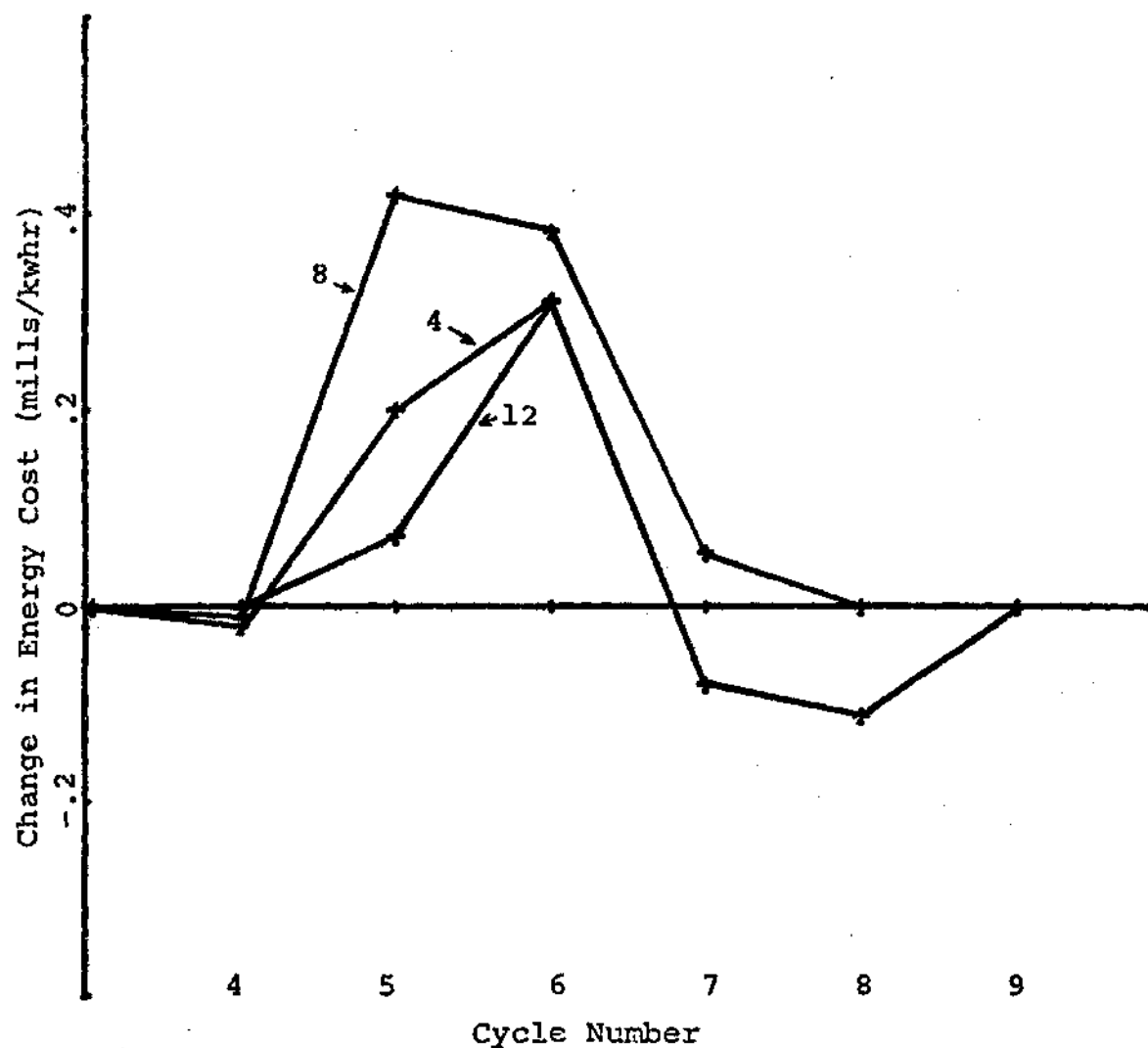


Figure 18. The Effect of Premature Fuel Discharge on Cycle Energy Costs
 Case 4--Discharge of 12 one-cycle low enrichment fuel assemblies
 Case 8--Discharge of 12 one-cycle high enrichment fuel assemblies
 Case 12--Discharge of 12 two-cycle high enrichment fuel assemblies

is the result of decreased fuel fabrication and reprocessing requirements when the three-cycle high enrichment fuel displaces two-cycle low enrichment fuel. The net effect over the five cycle period of perturbed operation is a 3.4% increase in energy costs. For Case 12, the predicted variations in fuel energy costs are identical to that of Case 4 with the exception of a slightly lower cycle energy cost for cycle 5 because of a smaller penalty for the discharge of the high enrichment fuel which has been irradiated for two cycles vs. the low enrichment fuel with one cycle of exposure. After the premature discharge of the fuel assemblies the subsequent core loadings are quite similar, and therefore energy production costs should also be approximately equal. The net energy cost variation for Case 12 is 1.2% greater than the base case energy cost over the five year period following the perturbed refueling.

Case 8 resulted in the highest total fuel cost and the perturbed refueling resulted in only a slight increase in fuel cycle length. Because of this, the cycle energy costs increased dramatically for the two cycles during which the replacement fuel for the early discharge was in core, but cost returned to the base case once the reactor core's contents reflected the equilibrium cycle fuel loading. The net increase in fuel costs for this case was 8%.

Analysis of the modified core simulator results to the problem under study lead to the following conclusions:

1. The early discharge of fuel can bring about large changes in cycle energy production because of variations in reactivity of reloaded cores. This effect is most severe in the cycle where the perturbation from the normal refueling scheme is first made and disappears quite rapidly once a return to the equilibrium cycle refueling plan is made.

2. Although the early discharge of fuel results in oscillations in energy production for subsequent cycles, the total energy production during the period of perturbed operation will remain very close to that produced during unperturbed operation. Even in the case of the worst variations in cycle energy, the total energy production for the perturbed cycles is negligible when compared to that of an equilibrium refueling scheme.

3. Although cycle energy production fluctuated as much as 15% for the cases under study, batch discharge exposure remained within 8% of the equilibrium discharge exposure values for all fuel except the batch which was discharged prematurely. Fluctuations in batch discharge exposure stabilize more quickly than cycle energy production. Because of this there is very little fluctuation in individual batch fuel costs except for the fuel batches which were prematurely discharged.

4. In terms of total batch fuel cost, the effect of increasing the number of fuel assemblies which were discharged early was a corresponding linear increase in

total fuel costs for the case. Early discharge high-enrichment assemblies after two cycles of operation is the least costly course of action, discharge of low enrichment assemblies after one cycle results in the next lower total cost, and the replacement of high enrichment assemblies after one cycle of irradiation results in the highest total batch fuel costs.

5. In terms of energy costs in mills/kwhr, none of the perturbations in reload patterns makes more than 8% difference in average fuel cycle cost over the period of perturbed operation for the discharge of up to twelve assemblies prematurely.

This application of the core simulator model showed its usefulness in analyzing "what-if" fuel management problems. Once the problem was stated, the necessary input information for a depletion analysis could be prepared in less than ten minutes. Reactor core depletion analyses were very inexpensive, requiring less than one second of CPU time on the Univac 1108. In short, this application shows that the core simulator model developed in this work is an accurate, quick-running, easy-to-use fuel management tool.

BIBLIOGRAPHY

1. Yankee Atomic Electric Company, Yankee Rowe, Final Hazards Summary Report.
2. Consolidated Edison, Indian Point, Final Hazards Summary Report.
3. Consumers Power Company, Palisades Point, Final Safety Analysis Report.
4. Commonwealth Edison, Dresden Station, Final Hazards Summary Report.
5. Consumer Power Company, Big Rock Point, Final Hazards Summary Report.
6. Pacific Gas and Electric Company, Humboldt Bay, Final Hazards Summary Report.
7. Civilian Power Reactor Program, Part II, Economic Potential and Development Programs TID-8517, 1959.
8. Civilian Power Reactor Program, Part III, Books 1 to 8, TID-8518, 1959.
9. S. Glasstone, A. Sesonske, Nuclear Reactor Engineering, 1967, pp. 714-749.
10. M. C. Edlund and G. K. Rhode, Nucleonics, Vol. 16, No. 5, p. 80, 1958.
11. C. Williams and R. T. Schomer, Proceedings Second U. N. Conference, Geneva, Vol. 9, p. 411, 1958.
12. Nucleonics, Vol. 18, No. 3, p. 108, 1960.
13. M. Novick and R. E. Rice, Proceedings Conference on Small and Medium Power Reactors, p. 111, IAEA, 1960.
14. L. A. Trilling, Proceedings Second U. N. Conference, Geneva, Vol. 9, p. 468, 1958.
15. L. D. P. King, Proceedings U. N. Conference, Geneva, Vol. 2, p. 372, 1956.

16. S. E. Beall and C. E. Winters, Chem. Eng. Prog., Vol. 50, p. 256, 1954.
17. S. E. Beall and J. A. Swartout, Proc. U. N. Conf., Geneva, Vol. 3, p. 263, 1956.
18. R. J. Thamer, et al., Proc. Second U. N. Conf., Geneva, Vol. 7, p. 54, 1958.
19. J. H. Devan, Trans. Am. Nuc. Soc., Vol. 4, p. 199, 1961.
20. Directory of Nuclear Reactors, Vol. 4, Vienna, 1962.
21. M. Benedict and T. H. Pigford, Nuclear Chemical Engineering, New York, 1957, p. 86-87.
22. G. J. Fischer, R. Avery, and B. J. Toppel, Fuel Cycle Analyses for Fast Power Breeder Reactors, Transactions of the American Nuclear Society, Vol. 5, No. 1, p. 130, 1962.
23. P. R. Kasten and L. L. Bennet, A Study of the Fuel Values of Pu and U-233, Transactions American Nuclear Society, Vol. 5, No. 1, 1962.
24. M. H. Chaffin, Status of the Market Nuclear Fuel Fabrication, NAC-33, July, 1973.
25. J. K. Pickard, Fuel Management and Supply Warranties Conference on Nuclear Fuel--Exploration to Power Reactors, Oklahoma City, May, 1961, p. 207-211.
26. W. H. Rowand, Fuel Policies of the System Supplier and Warrantor, Conference on Nuclear Fuel--Exploration to Power Reactors, Oklahoma City, May, 1968, p. 205-207.
27. David F. Shaw, Integration or Dis-integration in Nuclear Fuel Supply, Conference on Nuclear Fuel--Exploration to Power Reactors, Oklahoma City, May, 1968, p. 201-203.
28. G. R. Corey, A Flexible Buying Approach, Conference on Nuclear Fuel--Exploration to Power Reactors, Oklahoma City, May, 1968, p. 183-188.
29. E. A. Eschbach, QUICK--A Simplified Fuel Cost Code, HW-71812, January 2, 1962.
30. Royes Salmon, A Procedure and a Computer Code (POWERCO) for Calculating the Cost of Electricity Produced by Nuclear Power Stations, ORNL-3944, June, 1966.

31. Royes Salmon, Two Computer Codes (REFCO and POW76) for Calculating the Fuel Cycle Cost of a Nuclear Power Reactor, ORNL-4695, August, 1971.
32. F. W. Toot and J. R. Triplett, WAMPUM--A General Fuel Cycle Economics Code, GA-5316, October 27, 1965.
33. D. H. Lee, PWCOST, A General Purpose Computer Code for the Calculation of Fuel Cycle Costs, GA-9394, June 10, 1969.
34. R. E. Hoskins, E. G. Cooper, and J. G. Belitz, NUCBID, A Comprehensive Nuclear Fuel Economics Code for Utility Applications, IEEE Transactions, Vol. PAS-91, No. 1, January/February, 1972.
35. John A. Hughes and Daniel P. Hang, Development of Engineering Economic Basis to Analyze Nuclear Fuel Cycle Costs, Transactions of American Nuclear Society, pp. 48-50, June, 1972.
36. C. H. Bloomster, J. H. Nail, and D. R. Haffner, PACTOLUS: A Code for Computing Nuclear Power Costs, BNWL-1169, January, 1970.
37. T. W. Craig, CINCAS, A Nuclear Fuel Cycle Engineering Economy and Accounting Forecasting Code, Edlund-Shure-Zwiefel Report, November 15, 1968.
38. Personal Communication, R. L. Heiks, Director of Nuclear Fuel Supply, Consumer's Power Company, May, 1975.
39. E. T. Merrill, ALTHAEA: A One-Dimensional Two-Group Diffusion Code with an Effective Four-Group Burnup, BNWL-462, May, 1971.
40. B. N. Naft and A. Sesonske, Pressurized Water Reactor Optimal Fuel Management, Nuclear Technology, Vol. 14, p. 123-132, May, 1972.
41. P. Civita, P. Fornaciari, F. Gangemi, and T. Mazzanti, Best-6: A Flexible Tool for Optimization of Fuel Loading Strategies, Transactions ANS/ENS European Nuclear Conference, p. 383-384, April, 1975.
42. Hiroshi Matoda, J. Hercaeg, and A. Sesonske, Optimization of Refueling Schedule for Light Water Reactors, Transactions American Nuclear Society, Vol. 17, p. 307, November, 1973.

43. S. L. Forkner and S. R. Specker, An Algorithm for Determining Optimum Fuel Management Decisions with Generalized Cycle Requirements, Conference on Mathematical Models and Computational Techniques for Analysis of Nuclear Systems, April, 1973.
44. R. R. Henderson and D. J. Bauhs, Fuel Management Simulation Studies at Westinghouse, ORNL-TM-4443, January, 1974.
45. I. Wall and H. Fenech, The Application of Dynamic Programming to Fuel Management Optimization, Nuclear Science and Engineering, Vol. 22, p. 285-297, 1965.
46. P. Kazmersky, PODECKA--A Pseudo One-Dimensional Point Depletion Algorithm, ORNL-TM-4443, January, 1974.
47. P. J. Fulford and Alexander Sesonske, In-Core Fuel Management Optimization, Nuclear News, Vol. 13, p. 58-62, July, 1970.
48. R. W. Carlson, Personal Communication regarding FUELOPT, A Proprietary GNFC Fuel Cycle Scoping Code, April, 1975.
49. R. P. Omberg, HAFCO--A Code for Calculating the Cost of Reactor Operating Strategies, Hanford Engineering Development Laboratory Technical Report (to be published).
50. B. Snyder and E. E. Lewis, Optimal Control Rod Policies for an Operating Cycle of a Simulated Boiling Water Reactor Core, Conference on Mathematical Models and Computational Techniques for Analysis of Nuclear Systems, April, 1973.
51. J. T. Rhodes and P. J. Fulford, Operational Planning Model for Multi-Nuclear Unit Systems, Transactions of the American Nuclear Society, Vol. 14, No. 2, p. 492, 1971.
52. J. P. Kearney, H. Y. Watt, M. Benedict, and E. A. Mason, The Simulation and Optimization of Nuclear Fuel Reloading Decisions, ORNL-TM-4443, January, 1974.
53. R. L. Stover and A. Sesonske, Optimization of BWR Fuel Management Using an Accelerated Exhaustive Search Algorithm, Journal of Nuclear Energy, Vol. 23, p. 673-682, 1969.
54. J. R. Fagan and A. Sesonske, Optimal Fuel Replacement in Reactivity Limited Systems, Journal of Nuclear Energy, Vol. 23, p. 683-696, 1969.

55. J. M. Viebrock and D. K. Vogt, Effect of Fuel Failures on Potential Lost Capacity for U. S. Nuclear Power Plants, NAC-U-7405, December, 1974.
56. D. K. Vogt, The Effect of Fuel Problems on Energy Extraction from Nuclear Fuel, Nuclear Assurance Corporation, Atlanta, August, 1975.
57. B. Pershagen and E. Tenerz, Techniques for Core Design and Fuel Management in a Boiling Water Reactor, Fourth United Nations International Conference on the Peaceful Uses of Atomic Energy, A/CONF 148/P/312, May, 1971.
58. D. R. Vondy, et al., Discussion about the Nuclear Reactor Code CITATION Conference on Mathematical Models and Computational Techniques for Analyses of Nuclear Systems, CONF-710302, p. 983, 1971.
59. I. H. Gibson, G. Nash, and M. J. Marshall, UK LWR Reactor Physics Codes and their Validation, Transactions ANS/ENS European Nuclear Conference, p. 329-331, April, 1975.
60. A. Buono, M. Paoletti Gualandi, R. Guidotti, V. Marinelli, F. Pistella, and G. Testa, Feedback of Experience into Application of Core Evaluation Methods, Transactions ANS/ENS European Nuclear Conference, p. 331-332, April, 1975.
61. W. R. Caldwell, PDQ-7 Reference Manual, WAPD-TM-678, January, 1967.
62. R. L. Crowther, Burnup Analysis of Large Boiling Water Reactors, Proceedings of a Panel in Vienna, April, 1967, On Fuel Burnup Predictions in Thermal Reactors, IAEA, Vienna, 1968.
63. W. G. Flournoy, S. F. Deng, P. K. Shen, and R. P. Sullivan, Core Physics Calculations for San Onofre, Transaction of the American Nuclear Society, Vol. 17, p. 305-306, November, 1973.
64. R. J. Cacciapouti and V. N. Apelman, Core Physics Calculations for the Zircalloy-Stainless Core at Yankee, Transactions of the American Nuclear Society, Vol. 18, p. 177, June, 1974.
65. F. Todt, RELOAD FEVER--A One-Dimensional Few-Group Depletion Program for Fuel Cycle Analysis, GA-6612, September, 1965.

66. W. Kollmar, et al., Advanced In-Core Fuel Management for KWU LWR's: Criteria, Procedures, Results, Transactions ANS/ENS European Nuclear Conference, p. 386-387, April, 1975.
67. R. Bonalumi, M. M. Giorcelli, and G. Vimercati, COMETA: An Ultra-Coarse Mesh Three-Dimensional Diffusion Code, Transactions ANS/ENS European Nuclear Conference, p. 362-364, April, 1975.
68. O. J. Marlowe and P. A. Ombrello, CANDLE--A One-Dimensional Few-Group Depletion Code for the IBM-704, WAPD-TM-53, May, 1957.
69. J. B. Callaghan, L. M. Culpepper, J. G. Fairey, E. M. Gelbard, C. M. King, T. J. Lawton, O. J. Marlowe, and D. S. McCarty, TURBO--A Two-Dimensional Depletion Code for the IBM-704, WAPD-TM-95, November, 1957.
70. D. S. McCarty, C. M. King, J. T. Mandel, and H. P. Henderson, DRACO--A Three-Dimensional Few-Group Depletion Code for the IBM-704, WAPD-TM-137, December, 1958.
71. S. Hendly and R. Mangan, TURBO--A Two-Dimensional Few-Group Depletion Code for the IBM-7090, WCAP-6059, March, 1964.
72. S. Kaplan, O. J. Marlowe, and W. R. Caldwell, Equations and Programs for Solutions of the Newton Group Diffusion Equations by Synthesis Approximations, WAPD-TM-337, December, 1963, p. 1.
73. C. J. Pfeifer and F. R. Urbanus, ZIP-2, Synthesis Depletion Program, WAPD-TM-228, November, 1961.
74. S. Kaplan, et al., Application of Synthesis Techniques to Problems Including Time Dependence, Nuclear Science and Engineering, 18(3), 363.
75. J. E. Mayer, Synthesis of Three-Dimensional Power Shapes--Flux Weighting Techniques, WAPD-BT-4, pp. 39-41, October, 1951.
76. D. L. Delp, D. L. Fischer, J. M. Harriman, and M. J. Stedwell, FLARE--A Three-Dimensional Boiling Water Reactor Simulator, GEAP-4598, July, 1964.
77. R. K. Haling, Operating Strategy in Maintaining an Optimum Power Distribution Throughout Life, TID-7692, 1963.

78. P. Loizzo, RIBOT: A Physical Model for Light-Water Lattice Calculations, BNWL-735, February, 1968.
79. R. J. Thompson, JASON: A Reactor Cell Code for Fortran II or IV, BNWL-482, September, 1967.
80. R. Barry, LEOPARD--A Spectrum Dependent Non-Spatial Depletion Code for the IBM-7094, WCAP-3269-26, 1963.
81. C. G. Poncelet, LASER--A Depletion Program for Lattice Calculations Based on MUFT and THERMOS, WCAP-6073, 1966.
82. H. Bohl, E. M. Gelbard, and G. H. Ryan, MUFT-4, Fast Neutron Spectrum Code for the IBM-704, WAPD-TM-72, July, 1957.
83. H. Amster and Roland Suarez, The Calculation of Thermal Constants Averaged over a Wigner-Wilkins Flux Spectrum, Description of the SOFOCAT Code WAPD-TM-39, 1957.
84. T. Celnik and S. Kellman, Evaluation of Some Nuclear Calculation Methods for use in Plutonium Recycle, Transactions American Nuclear Society, Vol. 10, No. 1, June, 1967.
85. C. Poncelet, Burnup Physics of Heterogeneous Reactor Lattices, WCAP-6069, June, 1965.
86. H. C. Honeck, THERMOS--A Thermalization Transport Theory Code for Reactor Lattice Calculations, BNL-5826, 1961.
87. E. A. Eschbach, D. E. Deonici, and M. F. Kanninen, PROTEUS--A Computer Code to Extend Burnup Data from a Point Burn-up Code, BNWL-850, Battelle Northwest Labs, June, 1968.
88. L. Koch, P. Brand, A. Cricchio, D. Sommer, and B. Zaffiro, Isotopic Correlations, A New Tool in Fuel Management, Transactions ANS/ENS European Nuclear Conference, April, 1975.
89. D. L. Prezbindowski, Theory of Present and Future Safeguards Applications of Isotopic Ratios, BNWL-SA-4276, March, 1972.
90. N. E. Carter, Use of Isotopic Composition Data to Improve Reactor Calculation Techniques, BNWL-SA-4275, March, 1972.
91. Personal Communication, C. B. Woodhall, July, 1975.

92. Guide for Economic Evaluation of Nuclear Reactor Plant Designs, NUS-531, January, 1969.
93. A Guide to Nuclear Power Cost Evaluation, TID-7025, April 30, 1963.
94. Y. I. Chang, System 1 User's Manual, Nuclear Assurance Corporation, August, 1974.
95. S. D. Conte and C. de Boor, Elementary Numerical Analysis, Second Edition, p. 44.
96. J. R. Lamarsh, Nuclear Reactor Theory, p. 298-299, 1966.
97. Fuel Burnup Predictions in Thermal Reactors, p. 227-240, 1968.
98. Personal Communication, R.W. Carlson, May 1975.
99. W. J. Dixon, ed., BMD Biomedical Computer Programs, 1973, p. 387-396.